The Meteorological Office General Circulation Model

by

A. Gilchrist

Meteorological Office, Bracknell

1. Introduction

The Dynamical Climatology branch of the Meteorological Office uses a number of global grid-point models which have similar basic structures but differ in horizontal resolution, in the numberand disposition of levels in the vertical, and in the parameterisation of physical processes. Three models have been used in substantial time integrations. They are:

(i) a 5-layer model with horizontal resolution about 330 km and equal pressure interval in in the vertical. It has been applied mainly to general circulation and climate problems. (Corby et al. (1972) Gilchrist (1974) Rowntree (1975a)).

(ii) an 11-layer model with unequal vertical intervals and a horizontal resolution of about 220 km. The model is still under development; up to the present (September 1975) it has been used in about 6 medium-range forecasting integrations. (Rowntree (1971) Saker (1974 a,b,c)) .

(iii) a 13-layer model, similar to the 5-layer in horizontal resolution and in vertical resolution in the troposphere, but with additional levels in the stratosphere. It has been used for investigation of the stratosphere. (Newson (1974)).

The disposition of levels and layer boundaries are shown in Table 1.

Table 1

σ -values of levels and boundaries

	5-layer model		11-layer model		13-layer model	
	Level	Boundary	Level	Boundary	Level	Boundary
1.	.9	1.00	.987	1.00	.896	1.00
		.8		.975		.80
2.	.7		.937		.695	
		.6		.900		.60
3.	.5		.844		.493	
		.4		.790		.40
4.	.3		.718		.319	
		.2		.650		.25
5.	.1		.577		.196	
		0.0		.510		.15
6.			.436		.117	
				.370		.09
7.			.317		.074	
				.270		.06
8.			.230		.049	
				.195		.04
9.			.157		.032	
				.125		.025
10.			.089		.020	
				.060		.015
11.			.022		.011	
				0.0		.008
12.					.0058	
						.004
13.					.0015	
						0.0

For the 11 and 13-layer models the level and layer boundary sigma values are related by

$$\sigma_L = \frac{\sigma_B(\text{lower}) - \sigma_B(\text{upper})}{\ln \sigma_B(\text{lower}) - \ln \sigma_B(\text{upper})}$$

2. The finite difference formulation

The complete finite difference formulation of the 5-level model is set out in Corby et al. (1972). For the most part, the estimates used are straightforward and those need not be discussed further here. However some estimates differ from those used in other models and therefore merit special consideration.

Thus a problem arises in the estimation of the pressure gradient term in sigma coordinates. It is necessary to obtain $(\partial\phi/\partial x)_p$ where ϕ is the geopotential and we consider the x-direction only for purposes of illustration. This term is

$$\left(\frac{\partial\phi}{\partial x}\right)_\sigma + \frac{RT}{p}\left(\frac{\partial p}{\partial x}\right)_\sigma \qquad (1)$$

where p is the pressure, T the temperature and R the gas constant. The problem is that the required gradient is a small residual remaining after differencing two large terms, and unless they are estimated consistently, the overall truncation error for the term may be very severe. The form used in the Meteorological Office models is

$$\delta_x \overline{\phi}^x + R\overline{\overline{T}^x \delta_x \ln p_*}^x \qquad (2)$$

where

$$\delta_x A = \frac{1}{\Delta x}\left[A\left(x+\tfrac{\Delta x}{2}\right) - A\left(x-\tfrac{\Delta x}{2}\right)\right] \qquad (3)$$

and

$$\overline{A}^x = \frac{1}{2}\left[A\left(x+\tfrac{\Delta x}{2}\right) + A\left(x-\tfrac{\Delta x}{2}\right)\right] \qquad (4)$$

To justify this, we note that we need only deal with

$$\delta_x \phi + R\overline{T}^x \delta_x \ln p_* \qquad (5)$$

since the formula, consistent with its attempt to obtain low truncation error, is formulated in terms of the lowest possible grid length for the system.

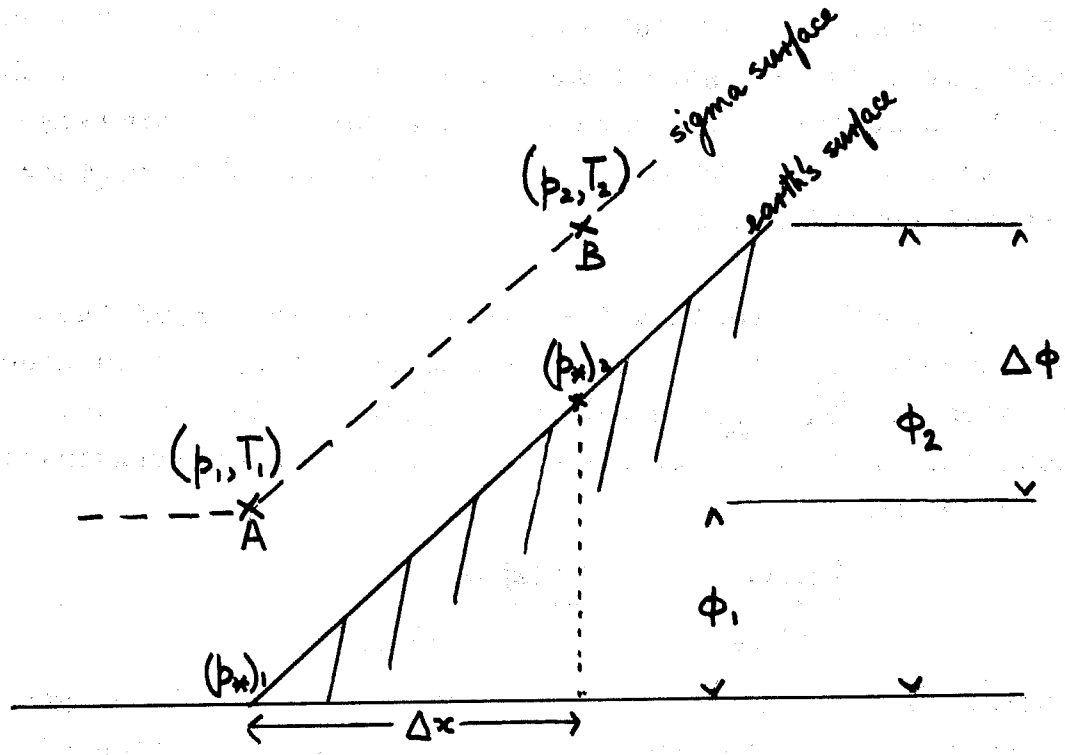

Figure 1

Consider an atmosphere in which there are no horizontal gradients but with topography which intersects the p-surfaces. (fig.1). Since the atmosphere is horizontally homogeneous, the horizontal differences in sigma surfaces may be replaced by vertical differences. Thus, $\Delta \propto \delta_x \phi$ applied to the conditions illustrated in fig. 1 is simply $\Delta\phi$, the difference in geopotential between points A and B, while $R\bar{T}^{*}\delta_x \ln p_*$ is $-R\left(\frac{T_1+T_2}{2}\right)\ln\left(p_1/p_2\right)$ which can also be recognised as an estimate of the same geopotential thickness with a negative sign; obviously, the two should cancel exactly. Analytically, this will happen when the atmosphere is such that $T = a\ln p + b$; $\bar{T}$ the mean temperature of the layer is $\left(\frac{T_1+T_2}{2}\right)$ i.e. the mean of the extreme values for which $\Delta\phi$ is required. In a finite difference model, it is most likely to happen when the integral form of the hydrostatic equation is taken as

$$(\Delta\phi)_{1,2} = R\left(\frac{T_1+T_2}{2}\right)\ln\frac{\sigma_1}{\sigma_2} \qquad (6)$$

when we can regard the model estimate of the pressure gradient term to be, in some sense, "ideal".

In the 5-level medium resolution model,(6) is taken as the formula for finding the geopotential at the levels at which the variables are carried i.e., we have

$$\phi_l = \phi_* + RT_n\ln\frac{1}{\sigma_n} + R\sum_{k=(n-1)}^{l}\frac{T_k+T_{k+1}}{2}\ln\frac{\sigma_{k+1}}{\sigma_k} \qquad (7)$$

where ϕ_* is the geopotential height of the earth's surface while the subscript indicates the model level and varies from 1 for the uppermost level to n for the lowest. Because unequal pressure intervals are involved in the vertical, the 11- and 13-layer models use

$$\phi_\ell = \phi_* + RT_\ell \ln \frac{\sigma_{\ell+\frac{1}{2}}}{\sigma_\ell} + R\sum_{k=n}^{\ell+1} T_k \ln \frac{\sigma_{k+\frac{1}{2}}}{\sigma_{k-\frac{1}{2}}} \qquad (8)$$

where the subscript $(k+\frac{1}{2})$ indicates the layer boundary situated between the levels k and (k+1). The difference between the values obtained by taking (7) and (8) is usually small under reasonable circumstances and no undesirable consequences resulting from the use of (8) rather than the "ideal" form have been noticed.

The use of the form (2) in the momentum equations has enabled the models to cope with irregular topography without obvious difficulties; no problems of stability near mountains due to the pressure gradient term have been encountered since adopting it. As an example of the topographic gradients in the 5-level model fig. 2 shows a cross-section through one of the roughest areas, across the Andes at 19.5°S.

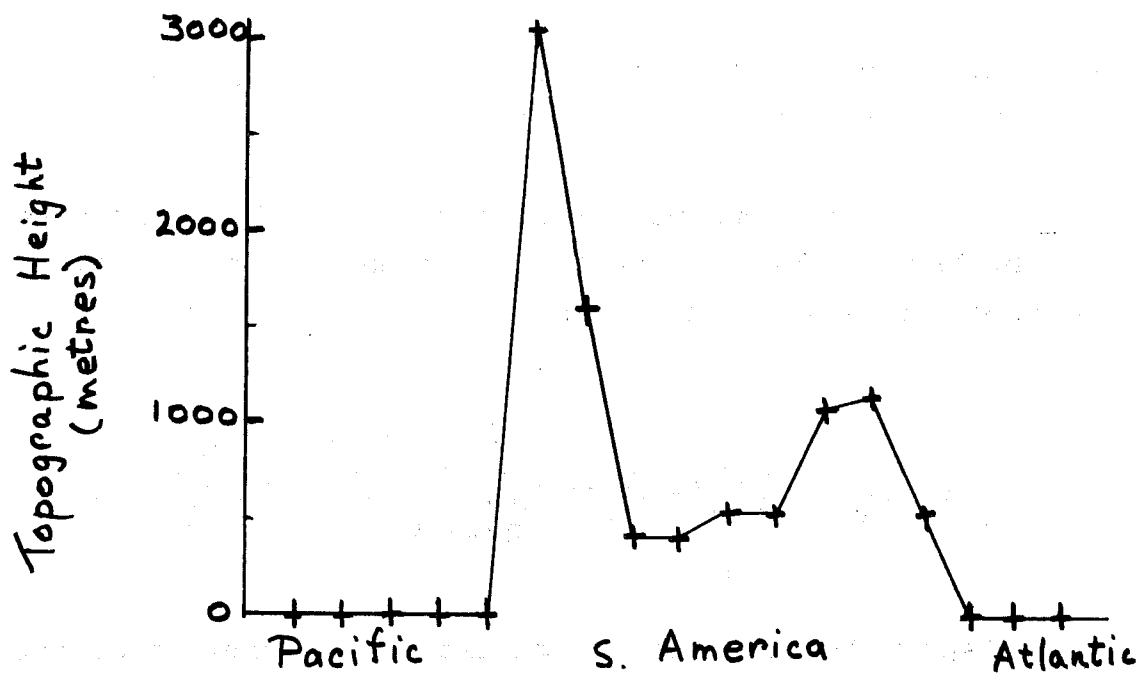

fig. 2

Next, consider the estimation of the 'ω' term in the thermodynamic equation. It is

$$-\frac{\kappa T \omega}{\sigma} = -\frac{\kappa T}{\sigma}\left(p_* \dot{\sigma} + \sigma \frac{\partial p_*}{\partial t} + \sigma \mathbf{V}\cdot\nabla p_*\right) ; \quad \kappa = \frac{R}{c_p} \qquad (9)$$

There is no obvious "best" estimate, and there are many possibilities. In Meteorological Office models it has been chosen to satisfy the finite difference requirement that the global integral of the energy conversion terms should be zero. Thus, the energy equation for the sigma system used in the models may be written in the absence of moisture and sources and sinks of energy

$$\frac{\partial E}{\partial t} + \nabla\cdot\mathbf{V}E + \frac{\partial}{\partial\sigma}\dot{\sigma}E + \frac{p_*}{g}\mathbf{V}\cdot\left(\nabla\phi + \frac{RT}{p_*}\nabla p_*\right) - \frac{RT\omega}{\sigma} = 0 \qquad (10)$$

where $E = \frac{p_*}{g}\left(\frac{\mathbf{V}^2}{2} + c_p T\right)$ and $\nabla\cdot$ and ∇ are respectively the 2-dimensional divergence and gradient operators. The second and third terms integrate to zero over the domain, while it is straightforward to show that the last two, the energy conversion terms, combine on integration to give $\phi_* \frac{\partial}{\partial t}(p_*/g)$ This is the change in potential energy due to redistribution of atmospheric mass over the earth's surface. The finite difference estimate for the ω term is therefore deduced algebraically from the requirement that the global integral of

$$\sum_{k=1}^{n}\left[p_* \mathbf{V}_k\cdot\{P.G.\} - \frac{RT\omega}{\sigma} - \phi_*\frac{\partial p_*}{\partial t}\right]\Delta\sigma_k \qquad (11)$$

where the summation is taken over all levels of the model, vanishes. The term (P.G.) in (11) is the finite difference estimate of the pressure gradient term based on (2). Now,

$$\frac{RT\omega}{\sigma} = -\frac{RT}{\sigma}\int_0^{\sigma} \nabla\cdot p_* \mathbb{V}\, d\sigma + RT\mathbb{V}\cdot\nabla p_* \qquad (12)$$

In order to combine with the pressure gradient term, whose finite difference expression has already been fixed, the last term in (12) has clearly to cancel with the second part of that estimate. That is, considering for illustration the x-direction only, $RT_k u_k \partial p_*/\partial x$ is to be estimated at level k by

$$u_k \overline{R\overline{T}_k^{x}\delta_x \ln p_*}^{x}$$

It is left to consider the expressions arising from the geopotential gradient along a sigma surface, which have the form

$$\sum_{k=1}^{n}\left[p_* u_k \cdot \delta_x \overline{\phi_k}^{x}\right]\Delta\sigma_k = \sum_{k=1}^{n}\left[p_* u_k\left(\delta_x\overline{\phi_*}^{x} + \sum_{l=k+1}^{n} a_l \delta_x \overline{T}_l^{x} + b_k \delta_x \overline{T}_k^{x}\right)\right]\Delta\sigma_k \qquad (13)$$

Using the integrated divergence equation in difference form (not derived here)

$$-\phi_* \frac{\partial p_*}{\partial t} = \phi_* \sum_{k=1}^{n} \delta_x \overline{p_* u_k}^{x}\cdot\Delta\sigma_k \qquad (14)$$

which combines with the first part of the R.H.S. of (13) to give

$$\sum_{k=1}^{n}\left(\delta_x \widetilde{p_* u_k \cdot \phi_*}^{x}\right)\cdot\Delta\sigma_k$$

(a) where $\widetilde{AB}^{x} = \frac{1}{2}\left[A\left(x+\frac{\Delta x}{2}\right)B\left(x-\frac{\Delta x}{2}\right) + \right.$ (15)

and we note that $\delta_x \widetilde{AB}^x = A\delta_x \overline{B}^x + B\delta_x \overline{A}^x$. An expression of this form vanishes on summation over a global domain.

The final terms in (13) can be written

$$\sum_{k=1}^{n} \delta_x \overline{T_k}^x \left[\sum_{l=1}^{k-1} a_k p_* u_l \Delta\sigma_l + b_k p_* w_k \Delta\sigma_k \right] \qquad (16)$$

The requirement that the global integral of the energy conversion terms is zero will then be met if the part of $-\frac{\kappa T \omega}{\sigma}$ derived from the integrated divergence (i.e. the first part of the right hand side of (12))satisfies

$$-\sum_{k=1}^{n} \left\{ \begin{matrix} \text{Integrated} \\ \text{divergence} \\ \text{estimate} \end{matrix} \right\}_k \Delta\sigma_k = +\kappa \sum_{k=1}^{n} T_k \left[\begin{matrix} \sum_{l=1}^{k-1} \frac{a_k \Delta\sigma_l}{\Delta\sigma_k} \delta_x \overline{p_* u_l}^x + \\ b_k \delta_x p_* w_k \end{matrix} \right] \Delta\sigma_k \qquad (17)$$

since then, on carrying out the summation indicated in (11), terms of the form (15) are produced. Hence we find the finite difference estimate for $-\frac{\kappa T_k \omega_k}{\sigma_k}$ written for one-dimension only is

$$\kappa \left[T_k \left\{ \frac{a_k}{\Delta\sigma_k} \sum_{l=1}^{k-1} \delta_x \overline{p_* u_l}^x \cdot \Delta\sigma_l + b_k \delta_x \overline{p_* u_k}^x \right\} - u_k \overline{\overline{T_k}^x \delta_x \ln p_*}^x \right] \qquad (18)$$

It will be observed that, in effect, $\frac{a_k}{\Delta\sigma_k}$ is an estimate of $\frac{1}{\sigma_k}$. For the 5-layer model using (7) it is, for the general term, $\frac{1}{2\Delta\sigma_k}\left(\ln\sigma_{k+1} / \ln\sigma_{k-1}\right)$ which can be recognised to be of the correct general character.

A similar problem to that of estimating the pressure gradient term near mountains occurs in the thermodynamic equation. In this case, the resultant temperature increment experienced by air as it is forced to ascend or descend by changes of topography is, in the simplest circumstances, the difference between the temperature change due to advection and that due to adiabatic expansion or contraction. These may be two large terms of opposite sign. Consider again the conditions of fig. 1 where in addition to the assumption of horizontal homogeneity already made we assume that the lapse rate is dry adiabatic. Motion must then be on sigma surfaces following the topography, and the temperature of the air should be invariant. Under the postulated circumstances the thermodynamic equation reduces to

$$\frac{\partial T}{\partial t} + u\left(\frac{\partial T}{\partial x} - \frac{\kappa T}{p_* \sigma}\frac{\partial p_*}{\partial x}\right) = 0 \qquad (19)$$

since $\dot{\sigma} = 0$ and $\frac{\partial p_*}{\partial t} = 0$. Note that $\frac{\kappa T}{p_* \sigma}$ is the adiabatic lapse rate per millibar and that the term in brackets may therefore be written

$$\frac{1}{\Delta x}\left[(T_2 - T_1) - \gamma_p (p_2 - p_1)\right] \qquad (20)$$

and the two parts should cancel under adiabatic conditions. Now the estimate of the second part has already been decided since it comes from the ω term. It is

$$\frac{1}{c_p}\left[R\bar{T}^{\kappa} S_x \ln p_*\right] \qquad (21)$$

and again we can observe that this is a height times the adiabatic lapse rate in geopotential units $\left(\frac{1}{c_p}\right).(T_2 - T_1) = \left(\frac{1}{c_p}\right)\Delta\phi$ where $\Delta\phi$ is the geopotential thickness between points A and B. Thus for cancellation of the two large terms to give zero truncation error in the same sense as already found for the pressure gradient, it is clear that the approximation to the

thermodynamic equation should be of the form

$$\frac{\partial \underline{T}}{\partial t} + u\left(\delta_x \overline{T}^x - \kappa \overline{T}^x \delta_x \ln p_*\right) = 0 \qquad (22)$$

To obtain a conserving form of the thermodynamic equation p_* times (22) is added to $\underline{T}$ times the continuity equation (of which the 'x-term' is $\delta_x \overline{p_* u}^x$) giving

$$\frac{\partial}{\partial t} p_* \underline{T} + \delta_x \widetilde{p_* u . T}^x + \ldots\ldots = 0 \qquad (23)$$

The vertical advection of momentum, water vapour and temperature in the model's finite difference equations takes the form $\delta_\sigma (p_* \dot{\sigma}) \overline{X}^\sigma$ where X is the variable concerned and $\overline{X}^\sigma$ is taken to be its value on a layer boundary. Usually this is taken as simply the mean of the values in the upper and lower layers, but it is possible to define it as $\overline{X} = \mu X(\text{lower}) + (1-\mu) X(\text{upper})$ where μ is a weight (< 1) , and still retain linear (though not quadratic) conservation properties. It is particularly appropriate to use weights when the layers are of unequal depth and when dealing with quantities like q whose vertical distribution is highly non-linear. They are used in the 11-layer model for T and q; for temperature they give correct values on the boundary when the lapse rate is dry adiabatic while for specific humidity they allow for the climatological average vertical humidity lapse.

Only brief mention will be made of the terms used to represent the effects of sub-grid scale turbulence on the explicit motions. Most integrations with the models have retained the original form discussed by Corby et al. (1972), which is very convenient computationally. For a variable X it takes the non-linear form $K\left|\frac{1}{p_*}\nabla\cdot p_*\nabla X\right|\frac{1}{p_*}\nabla\cdot p_*\nabla X$ and it was applied in the first experiment to u, v, q and potential temperature. The extra computation required over that for the simple linear form is a "copy positive" and a multiplication. Other forms, which have theoretical advantages have been tried e.g. $K' = K\left\{\left(\frac{1}{p_*}\nabla\cdot p_*\nabla u\right)^2 + \left(\frac{1}{p_*}\nabla\cdot p_*\nabla v\right)^2\right\}^{1/2}$ applied to all variables and the deformation-dependent diffusion of Smagorinsky et al. (1965). While the results from these were good with no obvious disadvantages, equally it did not appear that they had any positive advantages. However, as a consequence of using the time filter described by Asselin (1972), it has been possible to use smaller values of K than in the first experiment. Some experiments have also used the linear filter of the kind advocated by Shapiro (1971) and with results reported by Francis (1975). There are problems where the height of the earth's surface changes sharply and in later integrations it has been found advantageous to filter PMSL (rather than the surface pressure p_*) and a linear combination of temperature and potential temperature in preference to temperature alone.

3. The Horizontal Grid

The grid is chosen so as to give an approximately even distribution of points over the globe. In general concept it follows Kurihara (1965), and uses the method of quadratic conservation discussed by Bryan (1966). The first use of the grid which ensures an almost even distribution of points over the sphere in Meteorological Office calculations was reported by Grimmer and Shaw (1967). The grid points are defined on a latitude longitude network, with the number of points around a line of latitude chosen to be proportional to the cosine of latitude, subject to a minimum value of 16. The 5 and 13-layer models have a grid-length of 3° at the Equator; the 11-layer model value is 2°. The numbers of points around a line of latitudes are then as follows :

Table 2

5 and 13-layer

Lat.	88½	85½	82½	79½	76½	73½	10½	7½	4½	1½
No. points	16	16	16	22	28	34	118	119	120	120

11-layer

Lat.	89	87	85	83	81	79	7	5	3	1
No. points	16	16	16	22	28	34	179	179	180	180

In dealing with a grid of this structure the typical situation which occurs when the equations are in flux form is the following:

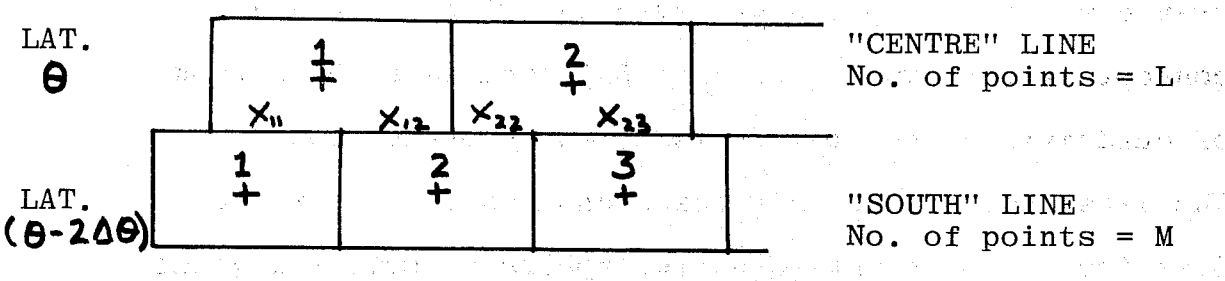

Fig. 3

where $X_{11}, X_{12}, X_{22}, X_{23}$, etc. are the fractions of the 'Centre' boxes overlapping the 'South' boxes, and the computation is essentially that of calculating fluxes (or terms computationally similar) between pairs of overlapping boxes with the appropriate weighting by the X's.

It may be of some interest to consider briefly the programming strategy that has been adopted to cope with this grid since it is fairly obvious that it can be very cumbersome to deal with unless care has been taken to achieve a conceptually simple and flexible computational plan. The programme proceeds as follows :

(i) a line of latitude is dealt with at a time

(ii) two lines of latitude are involved in the calculation at any one time. They can be thought of as the "Centre" (which is being updated) and the "South". The fluxes (or computationally similar terms) between them are stored so that

(ii) continued

they can be used on next entry to the routine when the "South" line has become "Centre". To conserve space, a "rolling" storage is used for the fluxes; in this they are overwritten as soon as they are no longer required for the calculation.

(iii) the situation illustrated in fig. 3 can be taken as applying either to the first boxes in a pair of lines or to the first boxes after a 'tri-box' situation has been dealt with (i.e. when one "Centre" box overlaps three to the "South"). Then with X_{11} given

$$X_{12} = 1 - X_{11} \; ; \; X_{22} = L/M - X_{12} \quad \text{etc.} \tag{24}$$

The "tri-box" situation is detected from

$$X^*_{n+1,n+1} = L/M - X^*_{n,n+1} < 0 \tag{25}$$

when the fractions become

$$X_{n,n+1} = L/M \; ; \; X_{n,n+2} = 1 - X_{n,n} - X_{n,n+1} \; ; \; X_{n+1,n+2} = \frac{L}{M} - X_{n,n+2} \equiv X'_{11} \tag{26}$$

Thus the programme is such that, given the number of points around a line of latitude and the fractional overlap of the first boxes, the computation can proceed. The algorithm for finding the fractions is very simple and can be invoked with little or no computational penalty. Programmed in this

way the grid is very flexible; for example the same programme is applicable to either a regular or irregular array of points. Compared with a regular grid, there is a penalty to be paid in that (L+M) fluxes have to be calculated. However, this is usually much less than the penalty incurred by other devices to overcome the problem of representation on the sphere.

The flexibility of the computational scheme was invoked in carrying out an experiment designed to show whether the performance of the grid could quickly be improved by increasing the minimum number of points around a line of latitude from 16 to a larger value. In the experiment the value taken was 64 forming a regular lat.-long. grid near the Pole. The number of points at the latitudes of the grid became as in Table 3.

Table 3

Lat.	89	87	85	83	81	79	77	75	73	71	69
Orig.	16	16	16	22	28	34	40	47	53	59	65
New	64	64	64	64	64	64	64	64	64	64	65
Trunc. wave No.	1	2	4	5	7	8	9	11	13	14	

The time-step was kept at its original value of 7½ minutes and linear computational stability was maintained by carrying out a Fourier transform of the p_*,u,v, and T values and truncating the representation at the wave-number shown in the last line of Table 3 after each time-step. (In normal computation with the grid using a minimum of 16 points, Fourier truncation is required for the two rows nearest the Pole). The mixing ratio values q were not truncated since experience has shown that this usually leads to computational instability due to the production of very low (or even negative) values. This computational scheme should achieve a considerable reduction of the type of truncation error near the Pole discussed by Shuman (1970).

The results of a forecast using this grid were compared with the forecast from the standard grid. Fig. 4 (a) and (b) shows the PMSL field over the northern part of the northern hemisphere at 3½ days from the initial time.

The mean and root mean square errors for the PMSL and 500 mb. height fields over the polar cap 70^{o} - 90^{o} N are shown in fig. 5 (a),(b),(c) and (d).

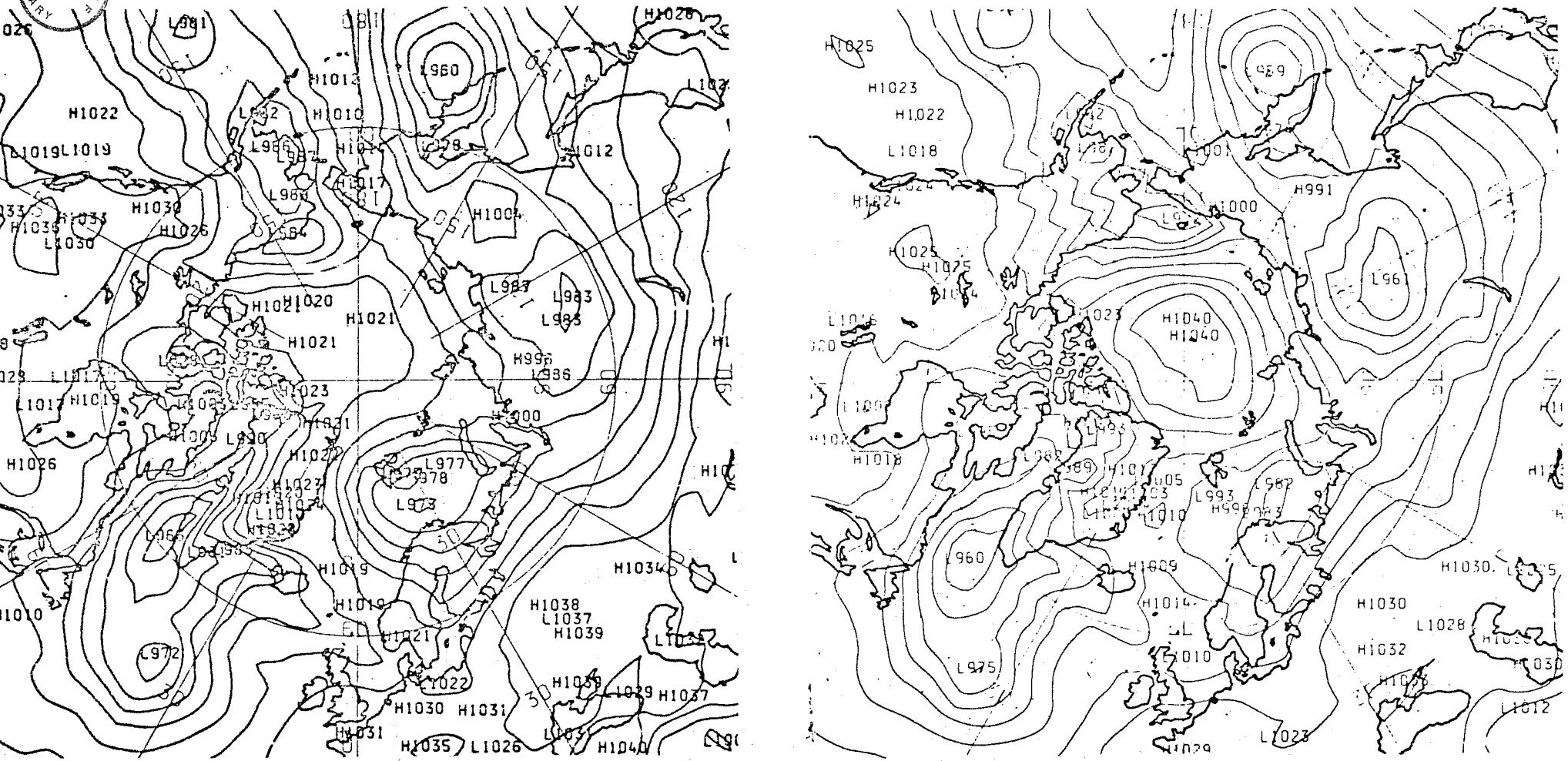

FIG. 4

PMSL FIELD AFTER 3 DAYS 12HR.

(a) STANDARD MODEL

(b) USING MINIMUM OF 64 POINTS

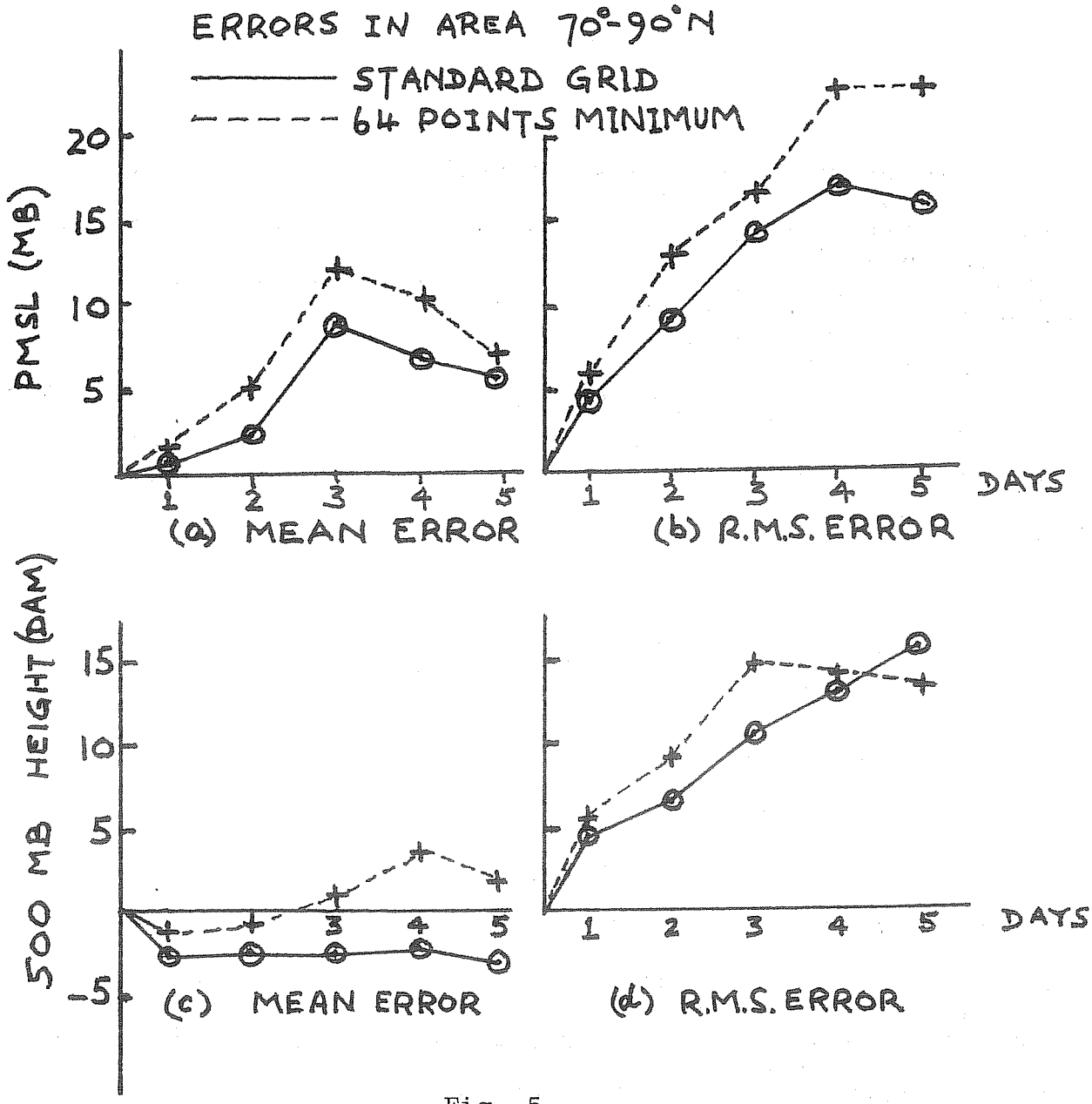

Fig. 5

It will be noted that for the particular initial conditions used on this occasion, the result of taking an increased number of points and applying Fourier truncation was to give errors that were significantly higher than those of the original grid. Despite the truncation, the higher resolution gave stronger gradients and rather more detail to the atmospheric structure, but since these were incorrect the overall results were worse.

On average the models all tend to produce too high pressure near the pole, but this is by no means a consistent effect; fairly low pressures and strong cross-polar flows also occur. The problem is probably a complicated one in which it is not to be too readily assumed that the only important contribution comes from the type of truncation we have been discussing.

4. Results of medium range forecasting experiments with the 11-layer model

The 11-layer model is still under development. In particular, investigation of the parameterisation schemes for convection, surface exchanges and radiation are proceeding, and are likely to lead to substantial changes. Because they are in a state of flux and since it is reasonable to suppose that they are not of crucial importance for forecasts of up to a few days ahead, only a short summary of the parameterisations will be attempted here.

(i) Surface exchanges. There are three model layers within the planetary boundary layer. For the surface exchanges and the boundary layer prescription, the proposals of Clarke (1970), type I are followed.

(ii) Convection. The scheme so far used follows that described by Corby et al. (1972). Some changes in detail are necessary because of the variable depth of model layers in the vertical.

(iii) Radiation. A full radiation calculation is performed every two hours of model time. The scheme is due to Hunt and Mattingly (1974) following a formulation which is closely akin to that of Manabe and Möller (1961). One layer of cloud was allowed, the fractional cloud cover being dependent on the relative humidity (Saker (1974 a)); any cloud was presumed to exist at the top of the boundary layer i.e. at sigma .844.

To provide a basis against which to evaluate any proposals for changing the parameterisations, medium range forecasts have been carried out from half a dozen initial conditions. Except for one data set which was created from hand analyses for the globe, the initial conditions were taken from the operational analyses produced at the Meteorological Office Central Forecast Office. These are not fully hemispheric and it has therefore been necessary to extend them by extrapolating to the equator. The model has generally been used in hemispheric form, with the exception that both hemispheric and global integrations have been carried out from the single global data set.

In order to carry out the integrations it was necessary first of all to initialise the data in some way. Temperton (1975) has experimented with the 5-layer model to try to determine what benefit was obtained by using various lengths of dynamic initialisation. The methodology consisted of interrupting an integration of the model, setting the divergence to zero (or nearly so) and continuing after varying amounts of initialisation (including none at all). The results were compared with an integration in which no interruption occurred. From the experiments he concluded that the forecasts after some time were very similar and very like the uninterrupted integration; differences showed little tendency to amplify. A similar conclusion as regards the effectiveness of dynamic initialisation was drawn by those responsible for running the U.K. Meteorological Office GATE forecast-analysis cycle (Lyne et al. (1975)). Temperton also found that dynamic initialisation did not restore the r.m.s. divergence,no matter how long it was carried on.

Thus the evidence seems to point to the conclusion that for forecasts in the medium-range period the method of initialisation is not of crucial importance, at least in general. (It may be noted that it is more important for some short range forecasts e.g. rainfall). In effect, it appears that gravity waves present in the initial data do not interact to a marked extent with the meteorological modes .
The initialisation used for forecasts with the 11-layer model has therefore been of a very simple form. The initial

data were available as heights of pressure surfaces. These were interpolated on to sigma surfaces and the linear balance equation solved directly to provide winds; in this, $\underline{f}$, the Coriolis parameter was kept constant from 21^{o}N to the equator, in order to avoid excessively strong winds at the most southerly lines of latitude.

Results of a forecast with the 11-layer model are illustrated in fig. 6-12. The initial conditions were for 12Z on 27th December 1972, this being the data set which was produced from hand drawn analyses. The model was run in hemispheric mode.

Fig. 6(a) and (b) show respectively the initial PMSL and 500 mb. contour charts. At 60hr. (fig. 7 (a)-(d)), the forecast has many realistic features and in general there is a good correlation between the predicted and actual positions and intensities of centres. However, although the wave-train to the north of the British Isles has the correct general shape, the phase is already substantially in error. Elsewhere, there are indications of errors which can be expected to have important consequences; for example, over the United States, the 500 mb. ridge is too weak.

Two days later (fig.8 (a)-(d)), errors are widespread and locally large. Probably the single worst feature is that the low over America, at about 90^{o}E in reality has been moved on by the model to be already over the Atlantic.

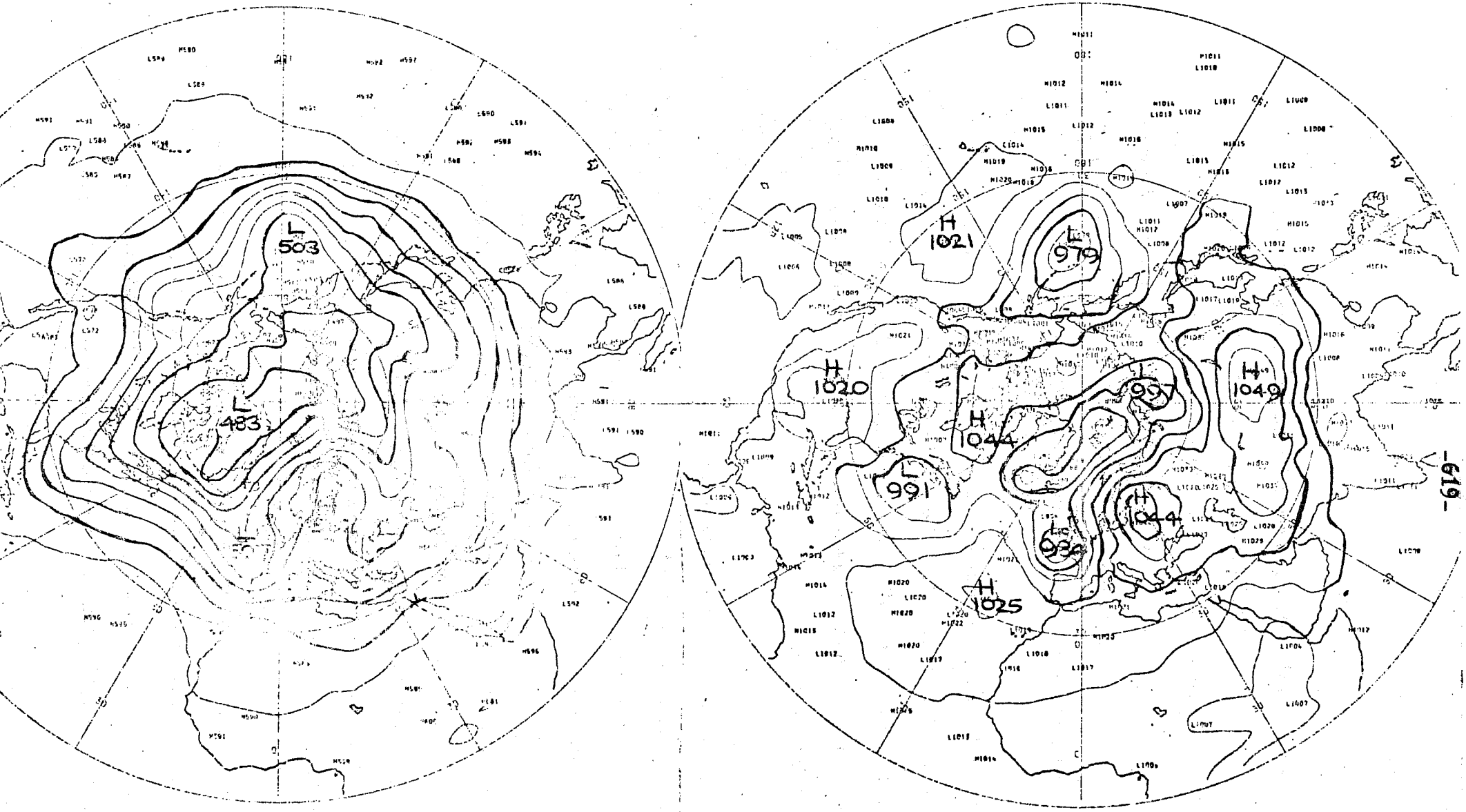

EXPERIMENT 10 TIME = 0000H12 500 MB HEIGHTS
CONTOUR INTERVAL = 12.00 DEKAMETRES

(b)

EXPERIMENT 10 TIME = 0000H12 PMSL
CONTOUR INTERVAL = 8.00 MB

(a)

INITIAL DATA 12Z 27/12/72
FIG. 6

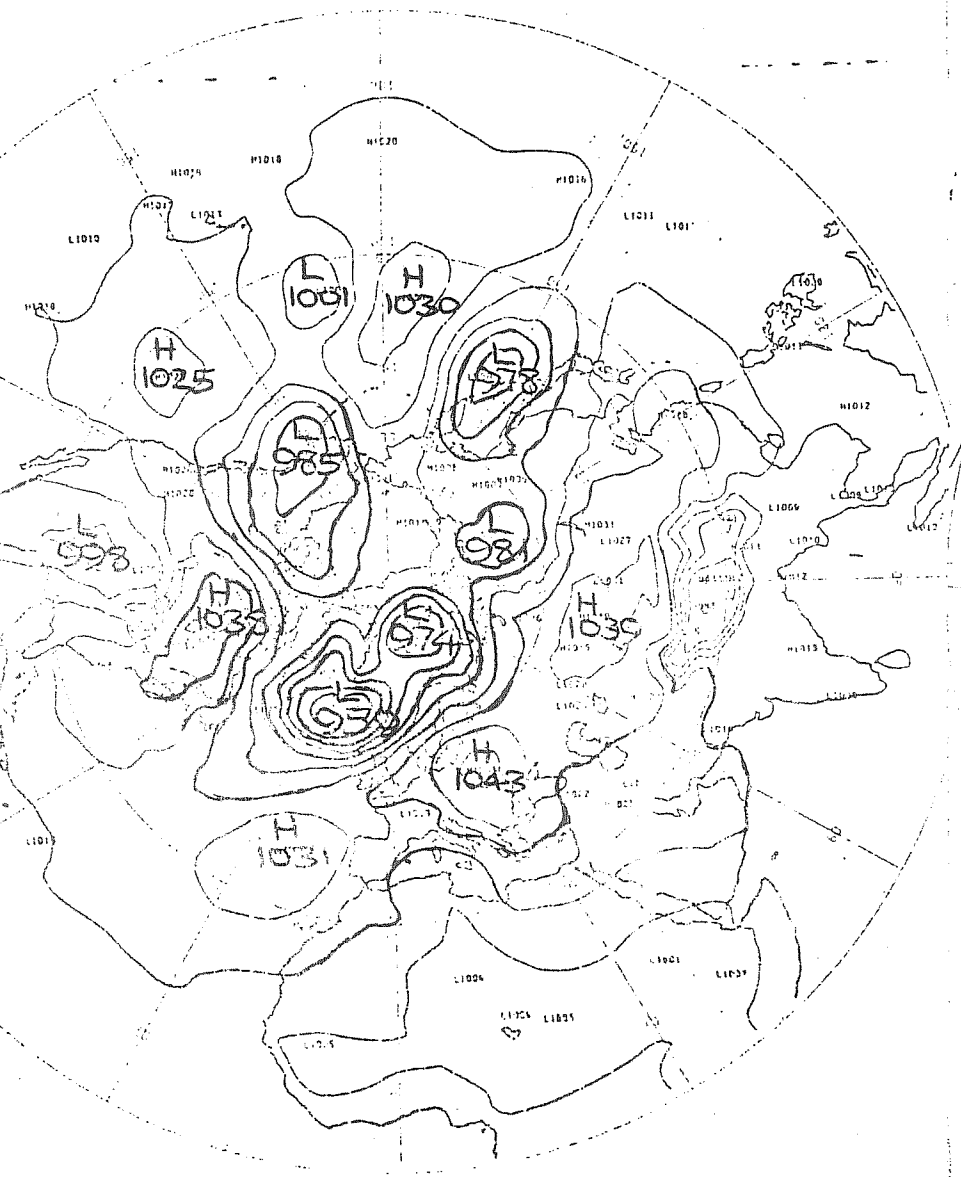

EXPERIMENT TIME = 0003H00 PMSL
CONTOUR INTERVAL = 8.00 MB

ACTUAL PMSL

(b)

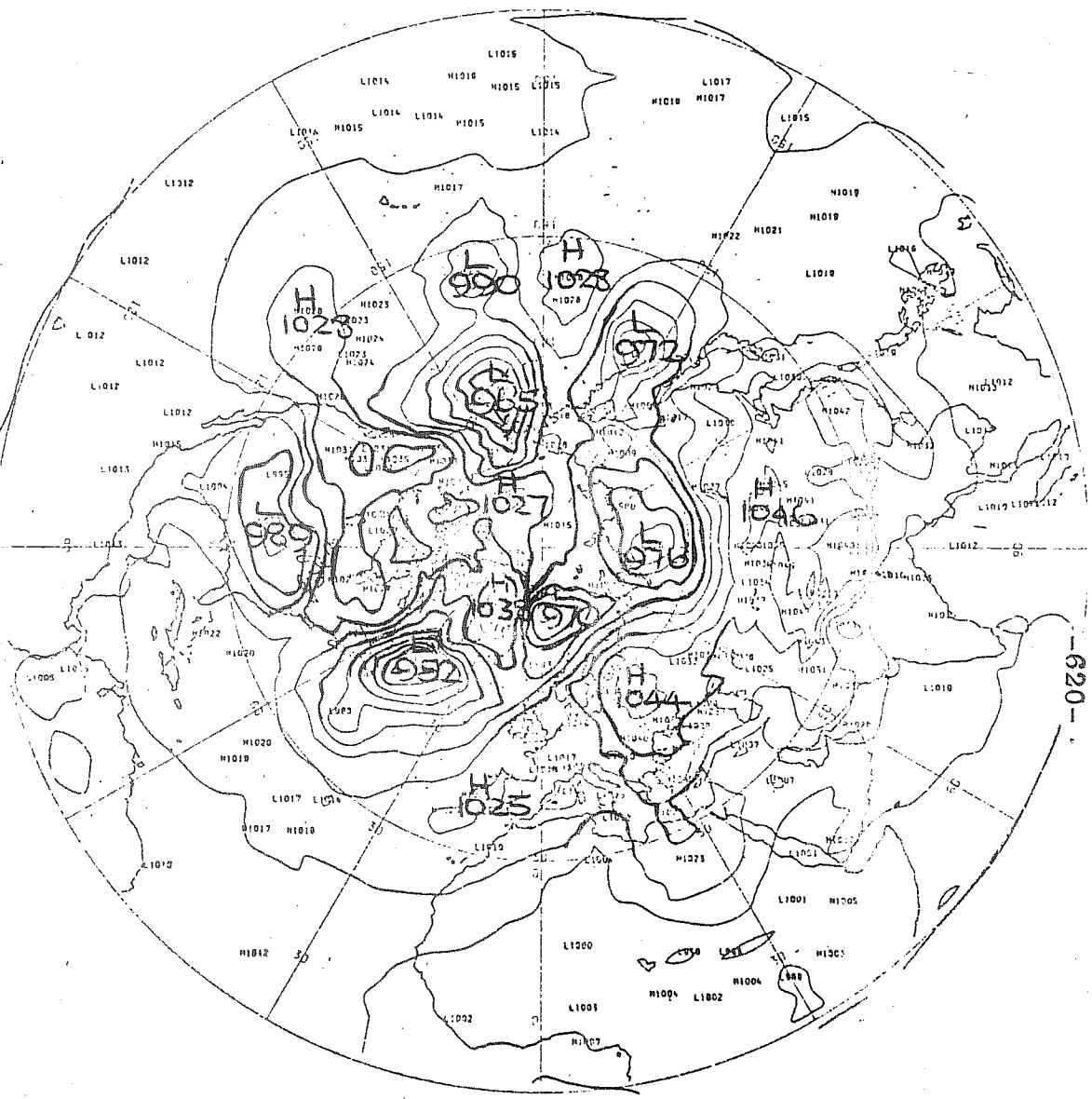

EXPERIMENT 10 TIME = 0003H00 PMSL
CONTOUR INTERVAL = 8.00 MB

PREDICTED PMSL

(a)

00Z 30/12/72

FIG. 7.

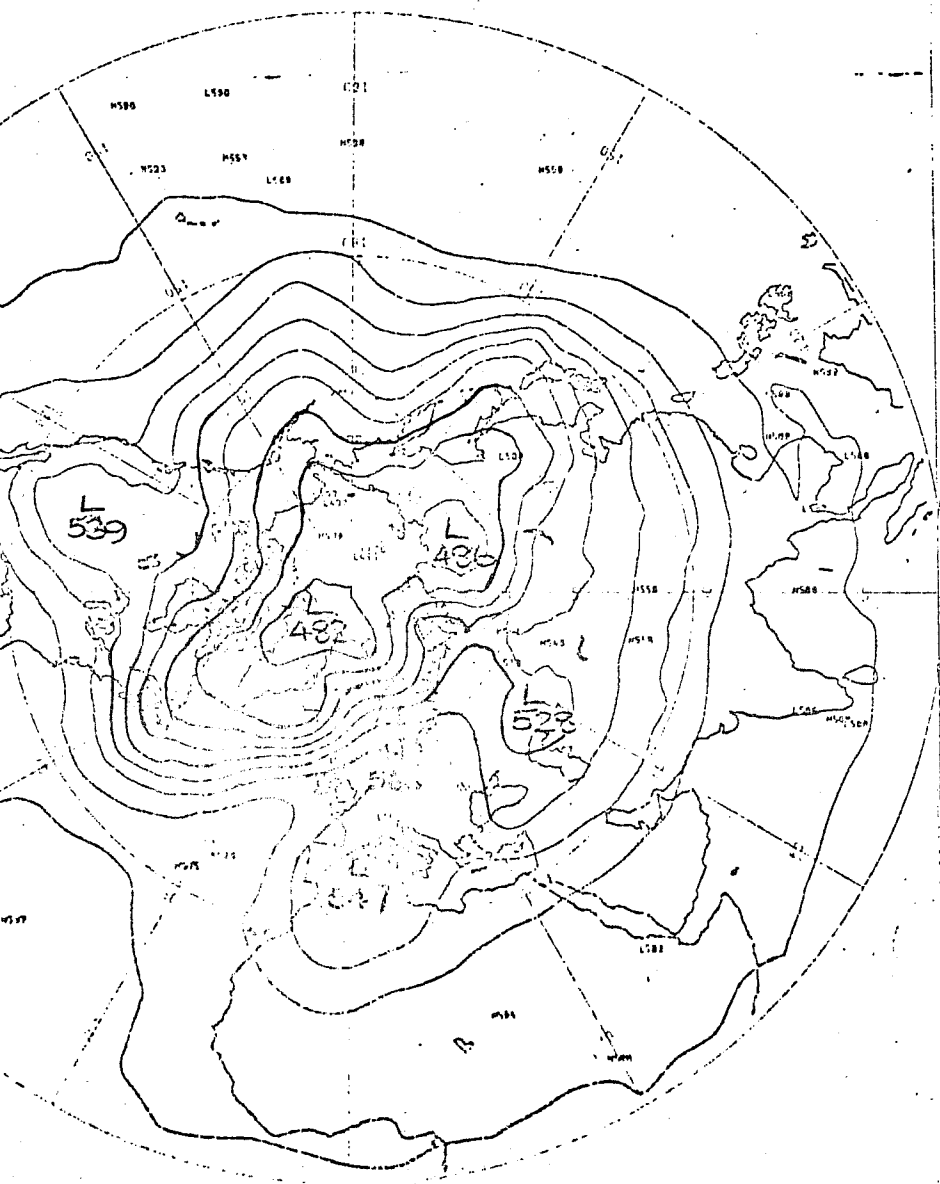

EXPERIMENT TIME = 0003400 500 MB HEIGHTS
CONTOUR INTERVAL = 12.00 DEKAMETRES

ACTUAL 500MB.
(a)

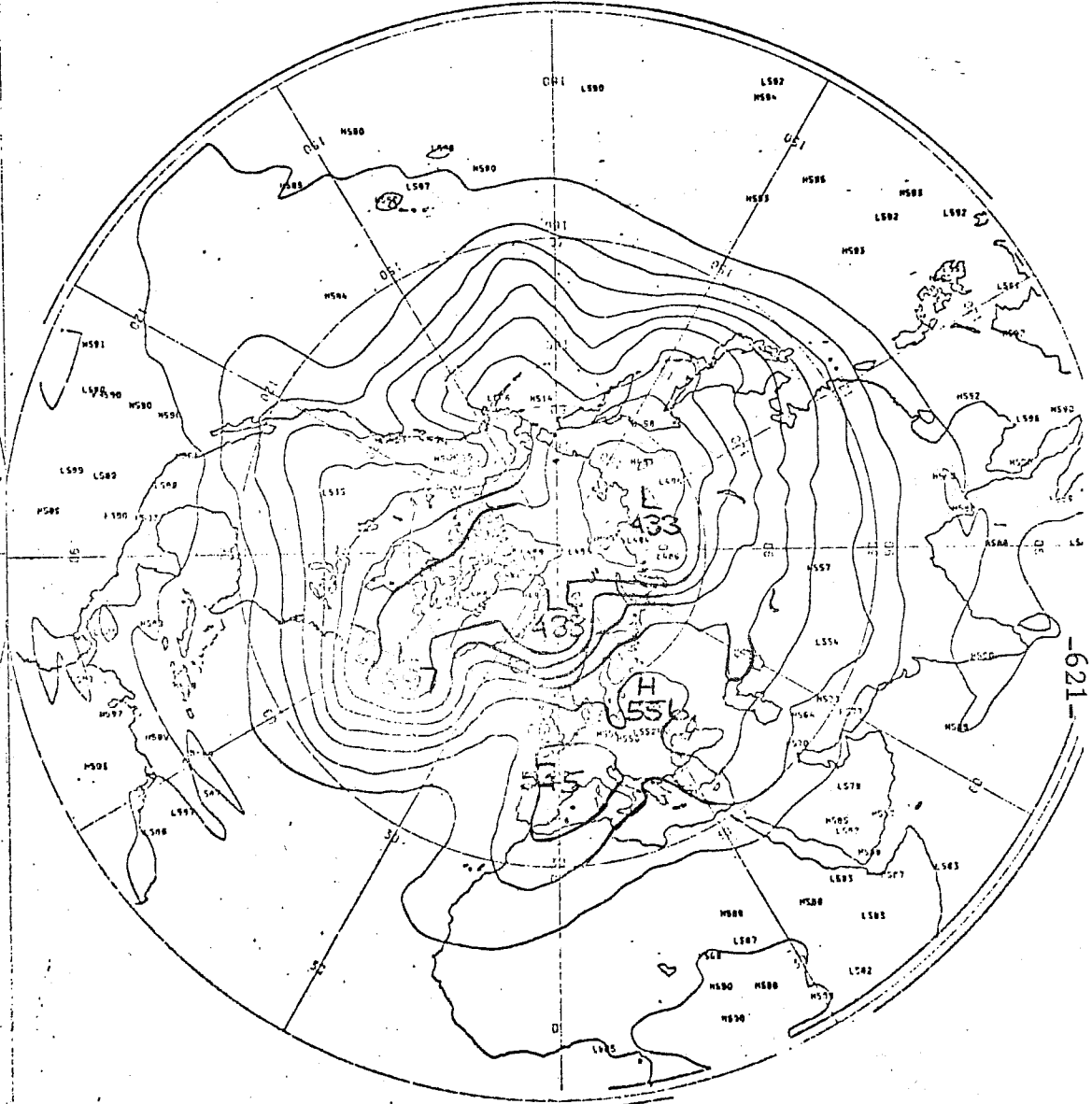

EXPERIMENT IC TIME = 0003400 500 MB HEIGHTS
CONTOUR INTERVAL = 12.00 DEKAMETRES

PREDICTED 500MB
(c)

00Z 30/12/72

FIG. 7.

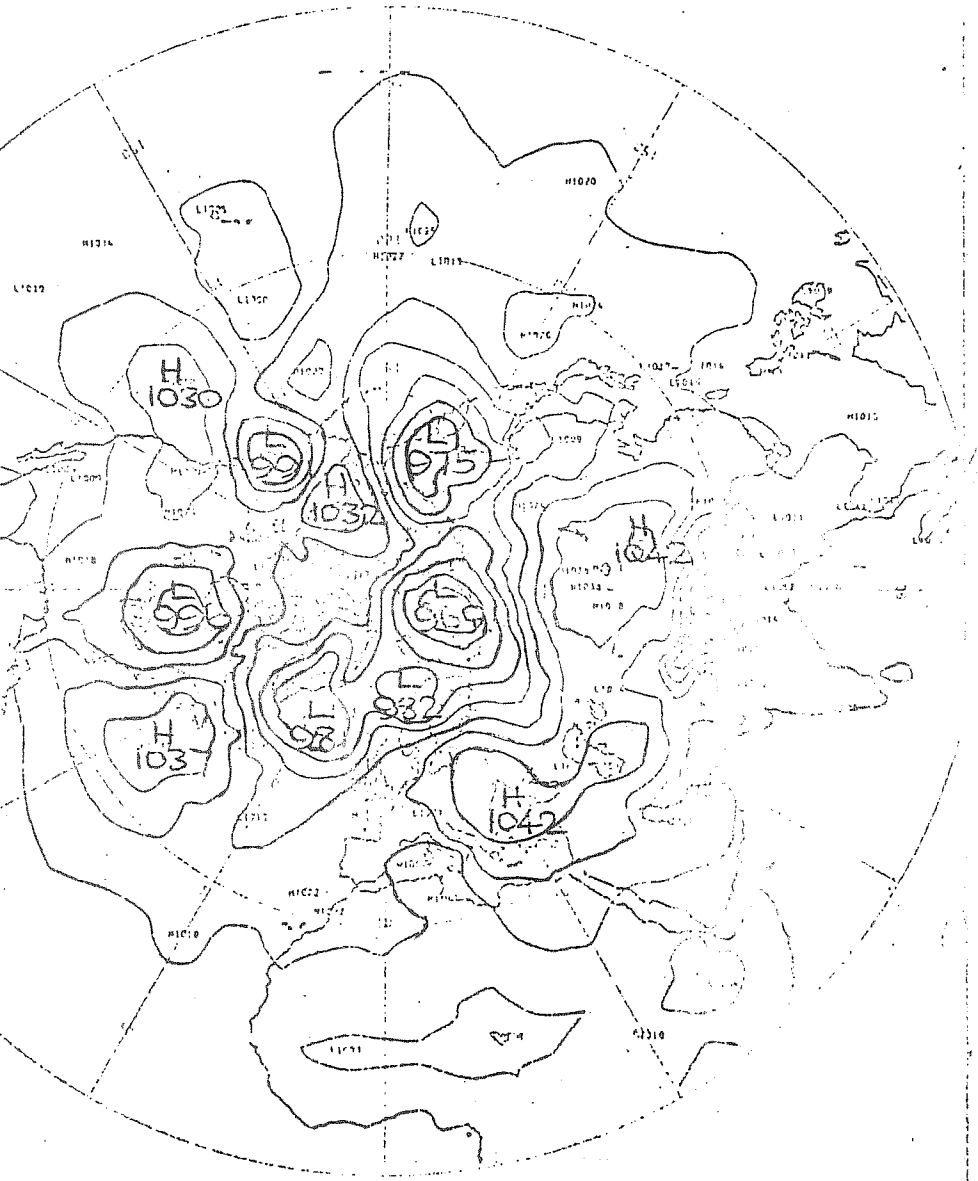

EXPERIMENT TIME = 000SH00 PMSL
CONTOUR INTERVAL = 8.00 MB

ACTUAL PMSL

(b)

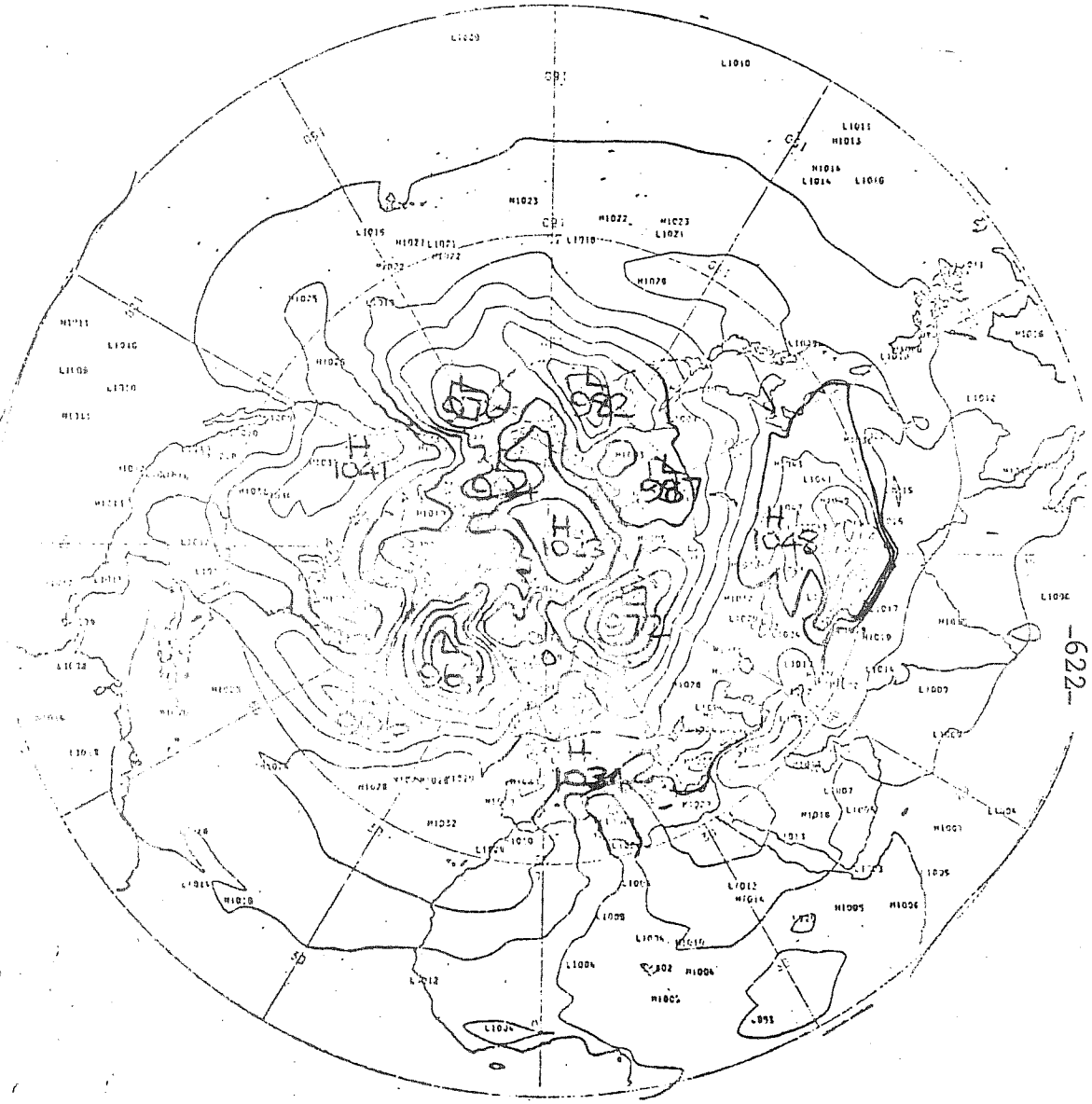

EXPERIMENT 10 TIME = 000SH00 PMSL
CONTOUR INTERVAL = 8.00 MB

PREDICTED PMSL

(a)

00Z 1/1/73

FIG. 8.

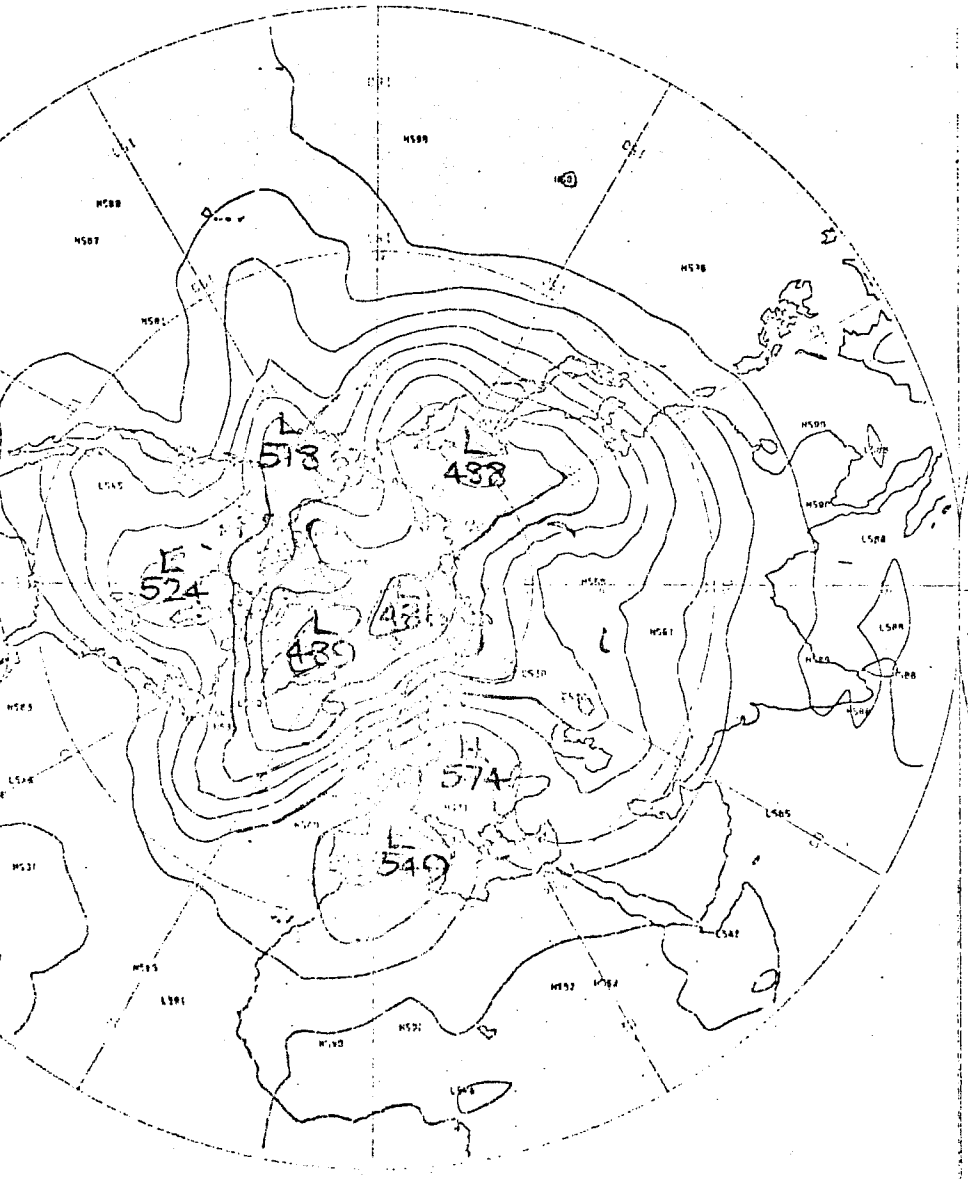

EXPERIMENT TIME = 000H00 500 MB HEIGHTS
CONTOUR INTERVAL = 12.00 DEKAMETRES

ACTUAL 500MB. 00Z 1/1/73
(d)

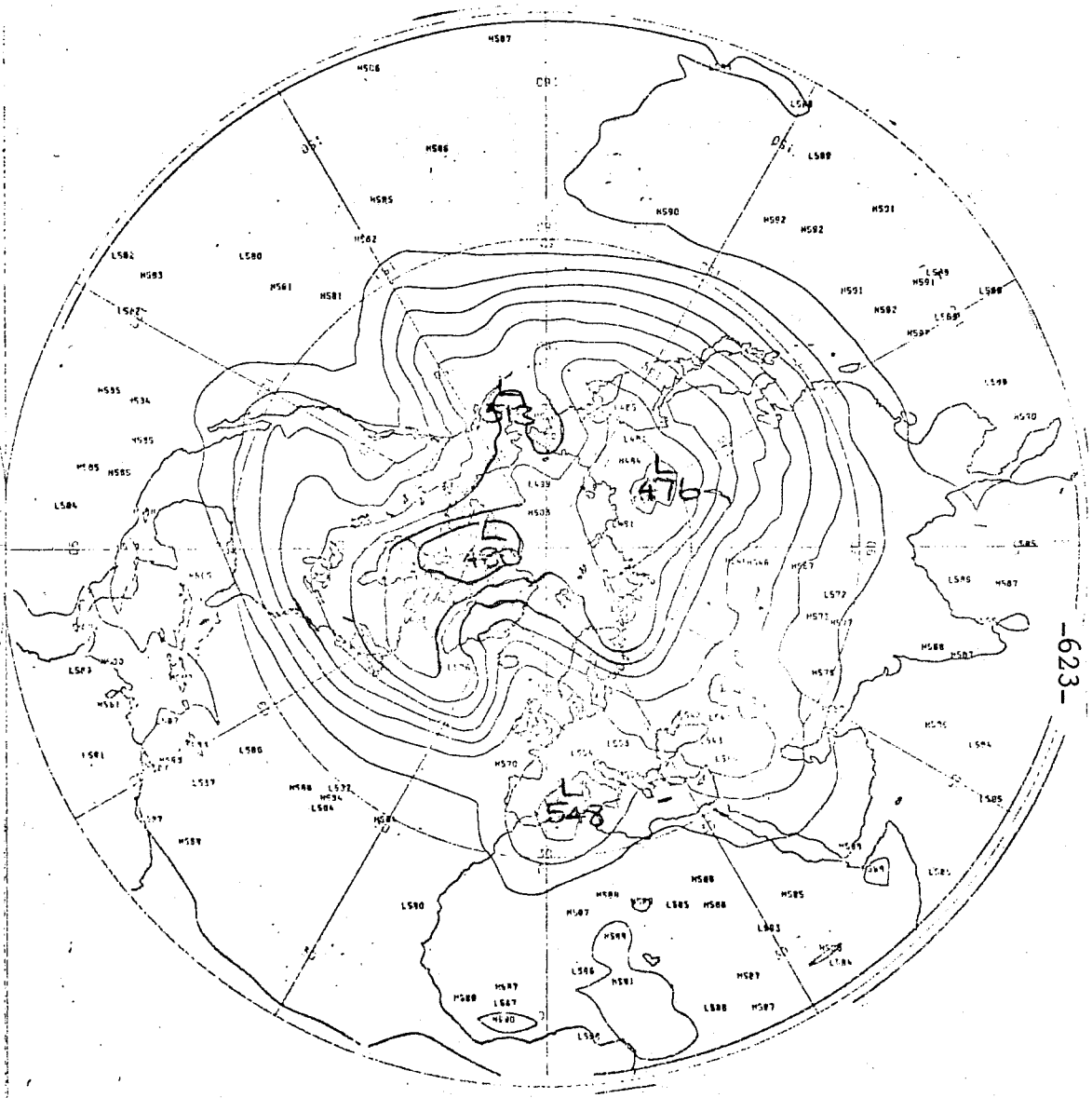

EXPERIMENT 10 TIME = 000H00 500 MB HEIGHTS
CONTOUR INTERVAL = 12.00 DEKAMETRES

PREDICTED 500 MB
(c)

FIG. 8

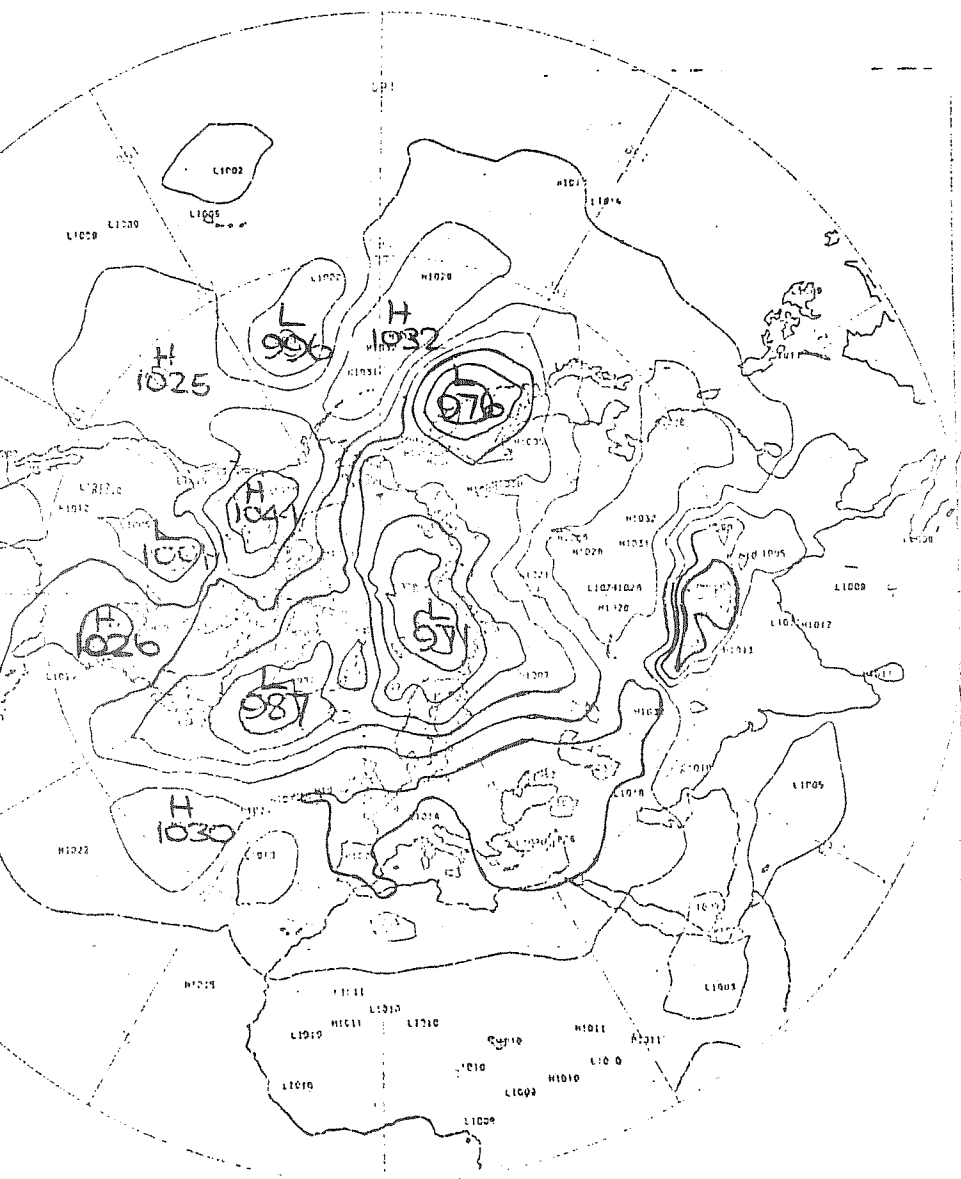

EXPERIMENT TIME = D007H00 PMSL
CONTOUR INTERVAL = 8.00 MB

ACTUAL PMSL

(a)

00Z 3/1/73

FIG. 9

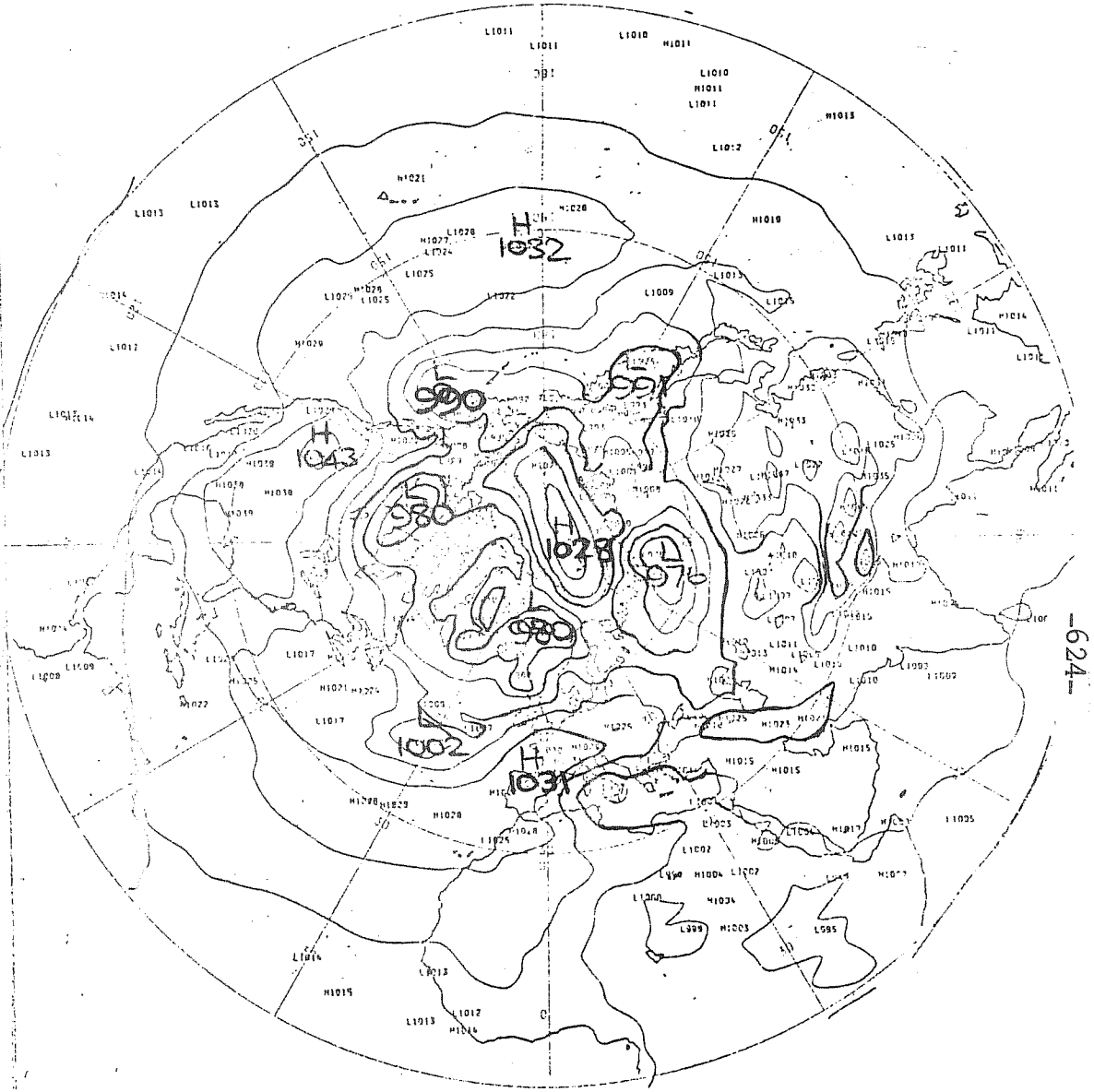

EXPERIMENT 10 TIME = D007H00 PMSL
CONTOUR INTERVAL = 8.00 MB

PREDICTED PMSL

(b)

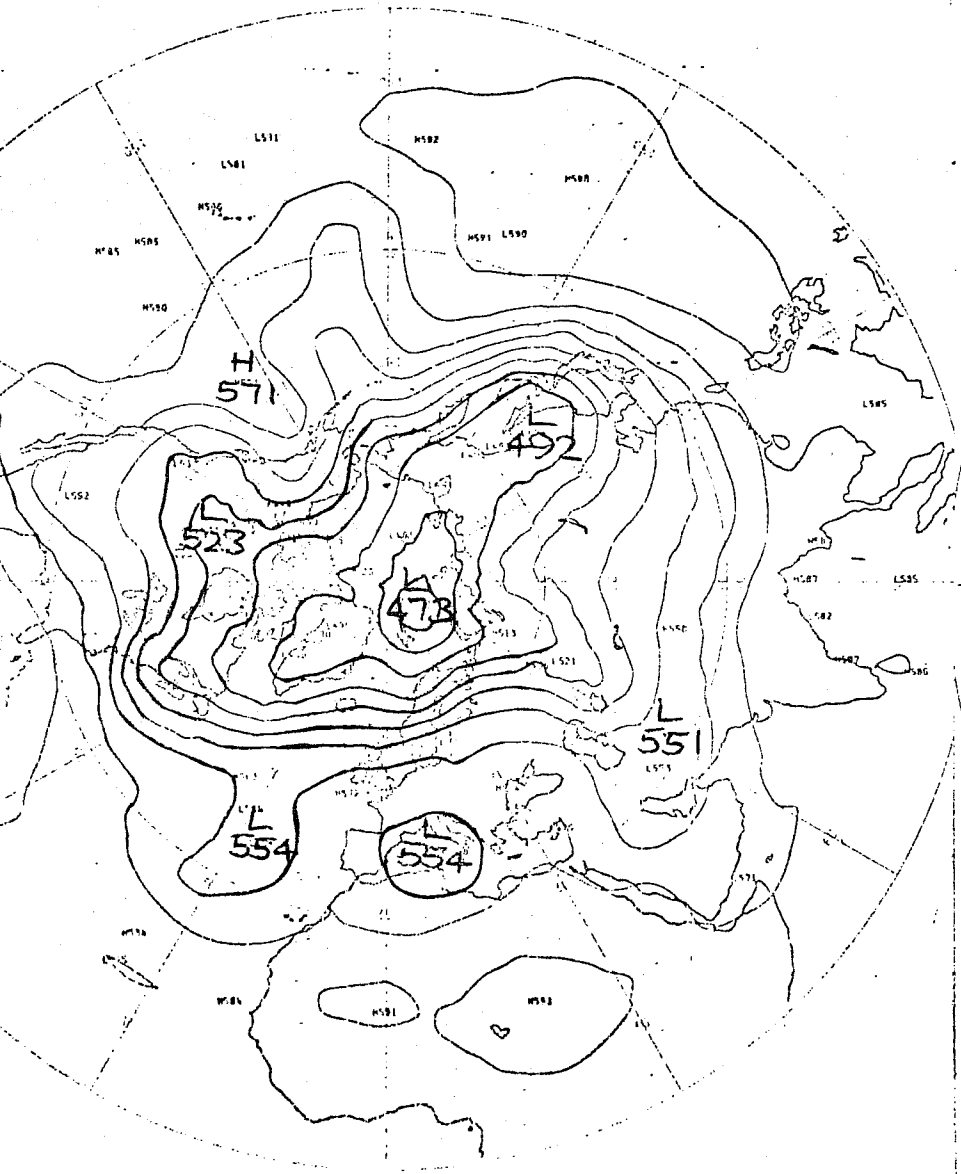

EXPERIMENT TIME = D007H00 500 MB HEIGHTS
CONTOUR INTERVAL = 12.00 DEKAMETRES

ACTUAL 500MB.
(d)

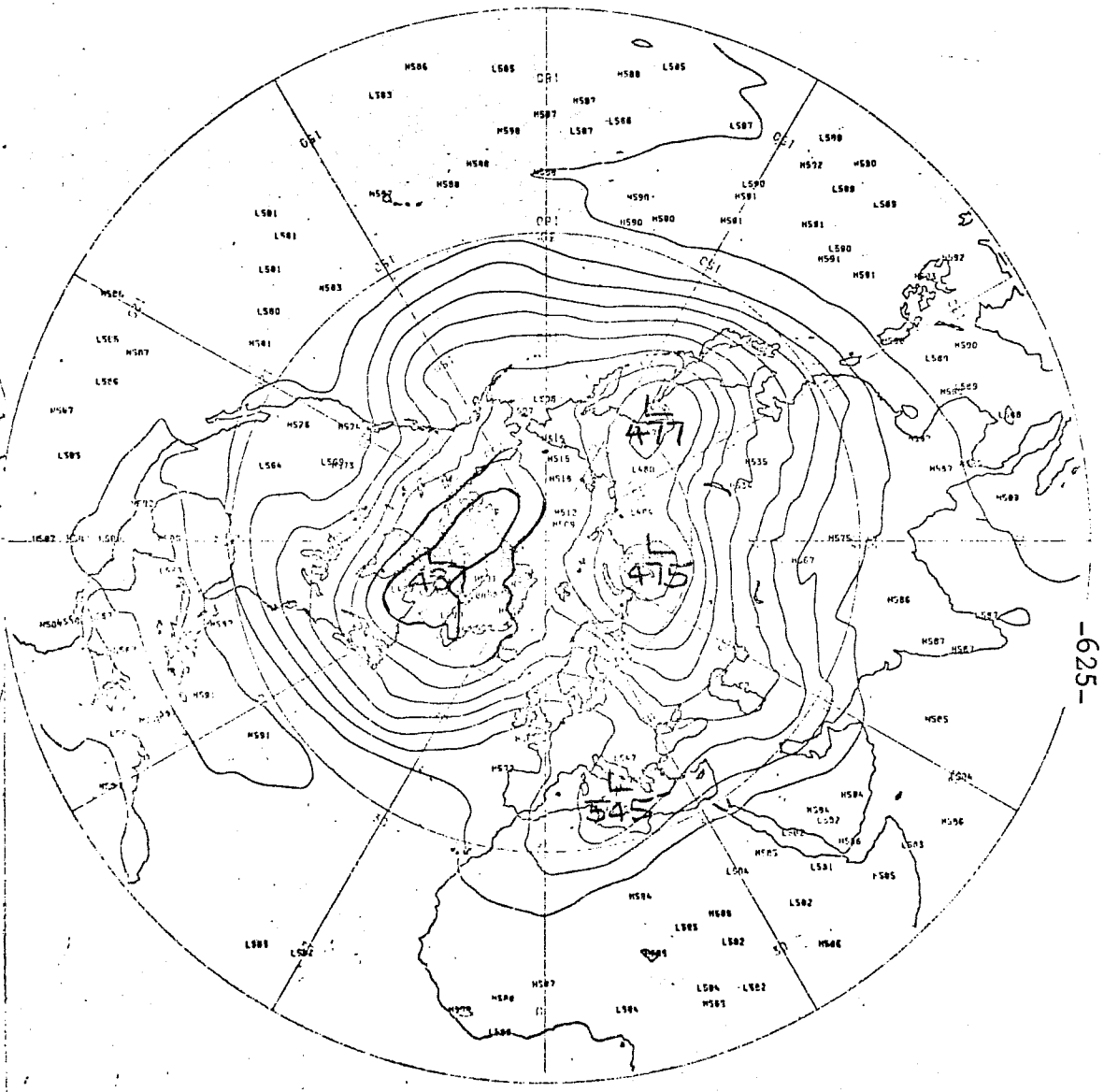

EXPERIMENT 10 TIME = D007H00 500 MB HEIGHTS
CONTOUR INTERVAL = 12.00 DEKAMETRES

PREDICTED 500MB
(c)

00Z 3/1/73

FIG. 9.

The 500 mb. flow is showing signs of lack of development. After another 48hr. (fig.9 (a)-(d)), there is probably little skill left in the forecast at least on the scale of depressions. In particular, one may observe that depressions which previously tended to be too deep are now significantly in error in the opposite sense. The 500 mb. flow is definitely too zonal.

It is instructive to look at the integration for particular wave-number groups on Hovmuller diagrams. Fig. 10, 11 and 12 show the reconstruction of the 500 mb. contour height field at latitude 41°N for waves 1-2, 3-5,and 6-10 respectively out to 7 days, for the model and as observed. For the two longest waves it is difficult to say whether or not the forecast has skill. The model apparently retains amplitude in the waves but the changes do not correspond well with observed values. However, perhaps the most important feature to note is that the initial conditions for the model (derived from hand-drawn analyses) do not correspond closely with those described as "observed", which were derived from operational analyses. The amplitudes and phases up to wave-number 10 are shown in Table 4.

HOVMOELLER TROUGH RIDGE DIAGRAM 500 mb

MEAN OF WAVE NOS 1 - 2 AT LATITUDE = 41

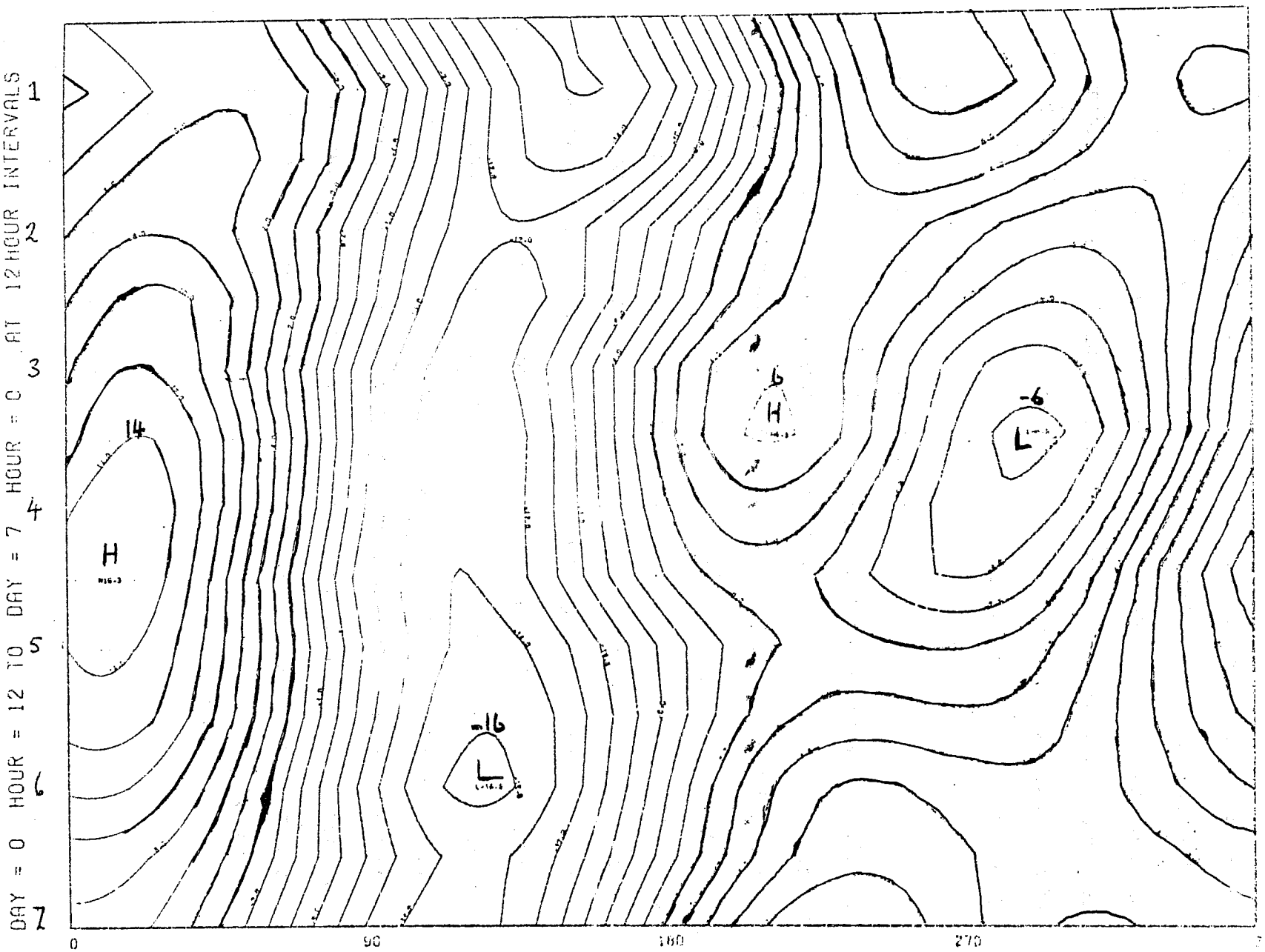

CONTOUR INTERVAL = 2.0

Experiment No. = 10

PREDICTED

FIG. 10(a)

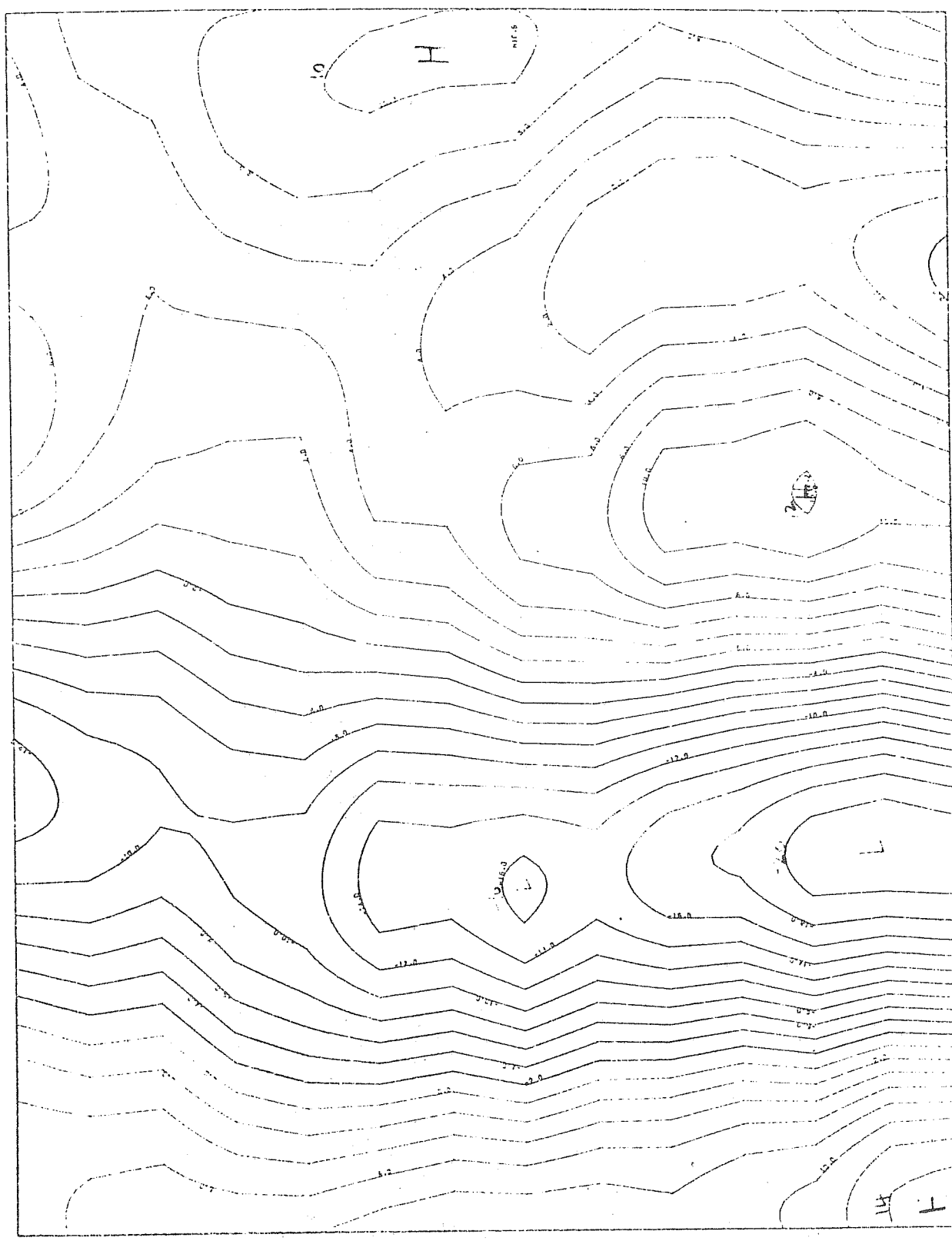

ACTUAL
FIG. 10(b)

PREDICTED

FIG. 11 (a)

HOVMOELLER TROUGH RIDGE DIAGRAM 500 MB.

MEAN OF WAVE NOS 3 - 5 AT LATITUDE = 41

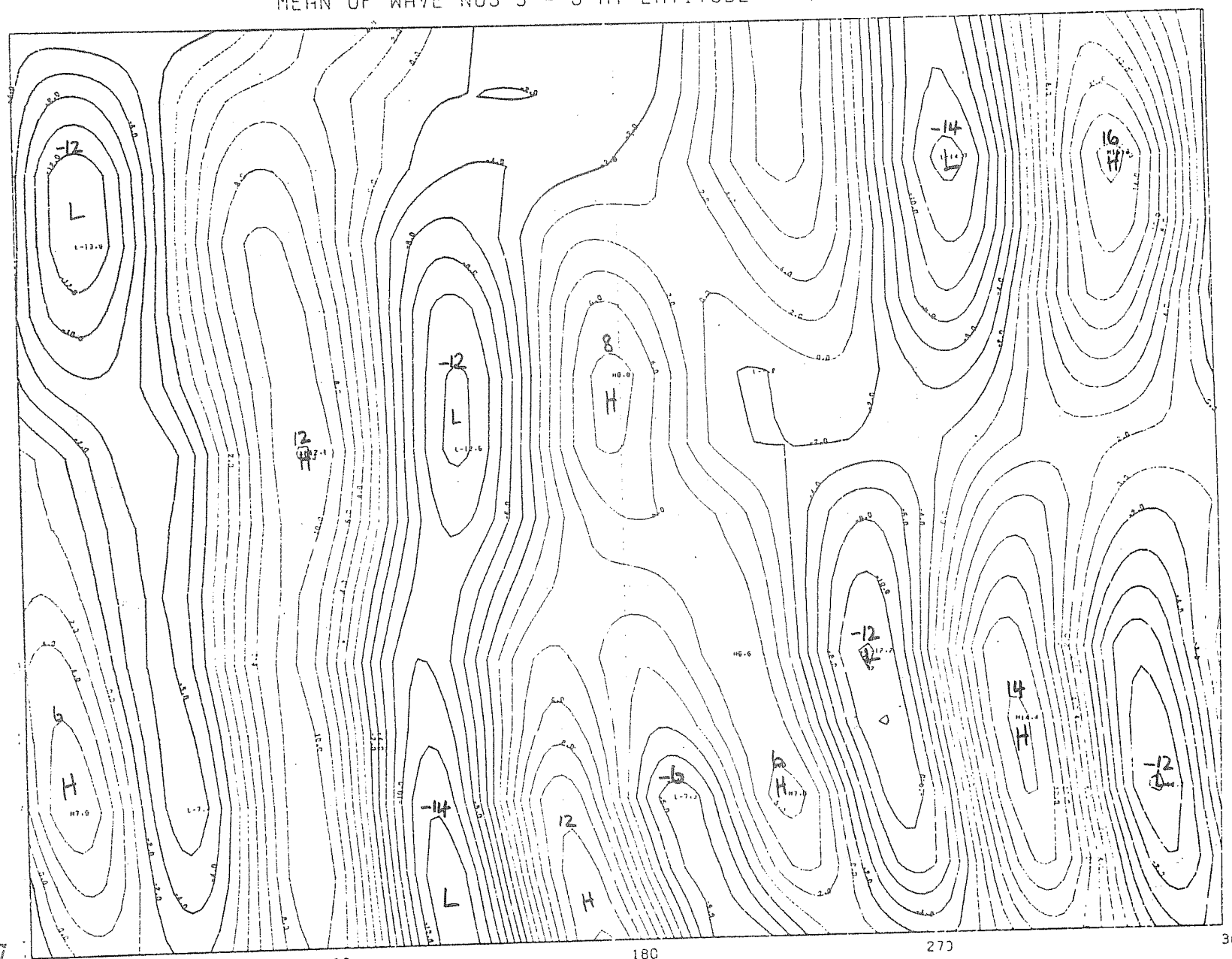

ACTUAL

FIG. 11(b)

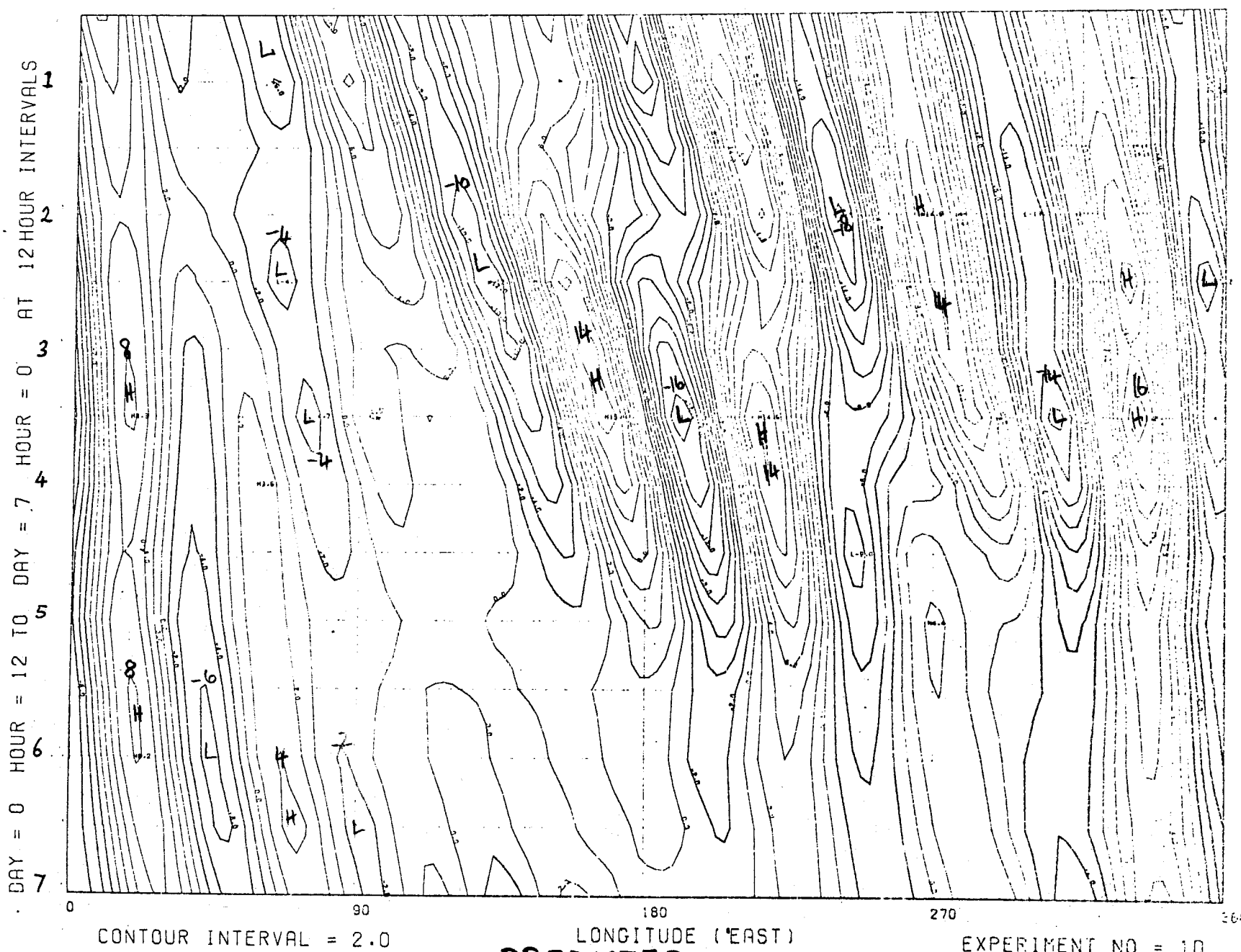

PREDICTED
FIG. 12 (a)

MEAN OF WAVE NOS 6 - 10 AT LATITUDE = 41

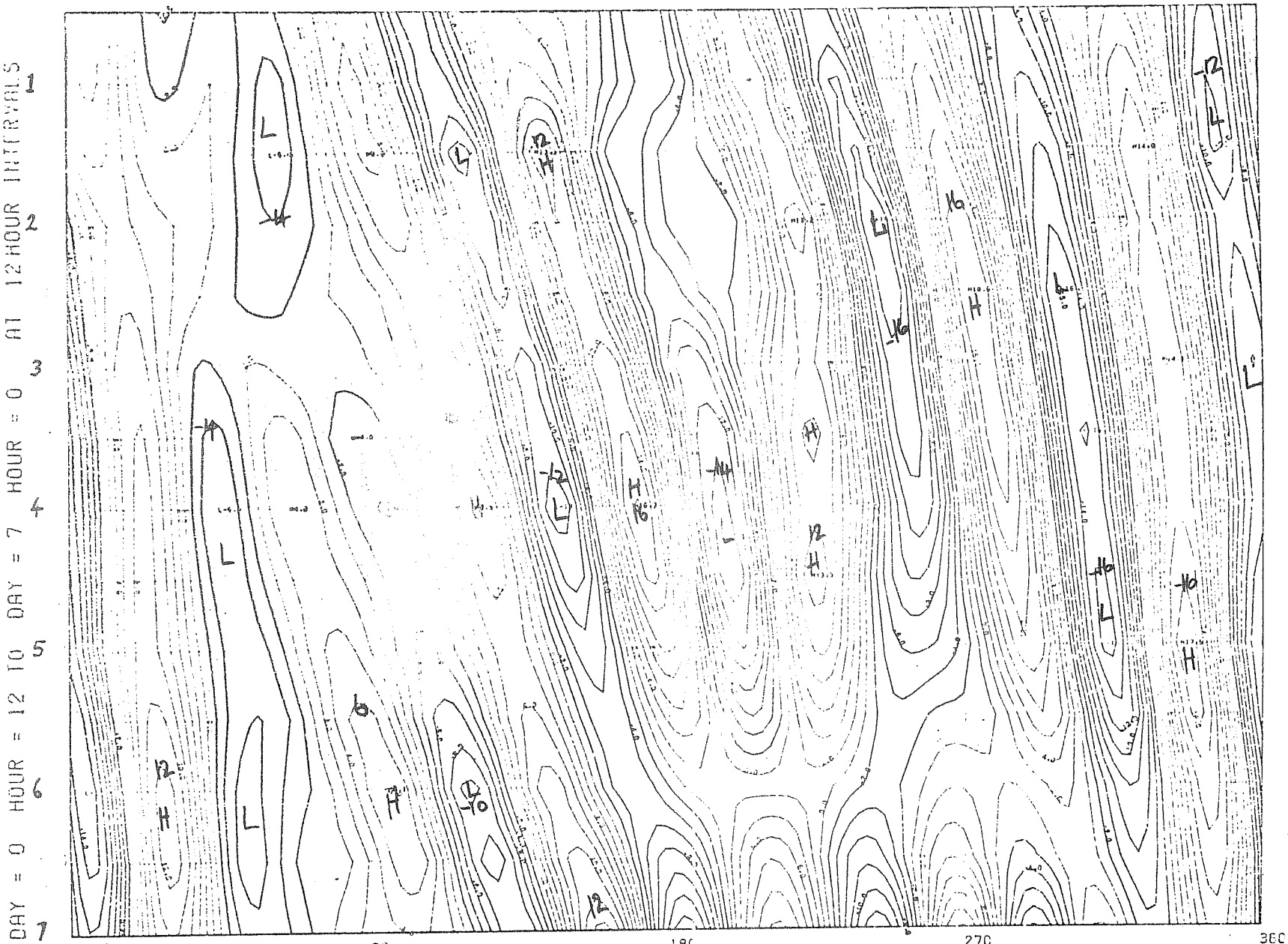

CONTOUR INTERVAL = 2.0

EXPERIMENT NO = 0

ACTUAL
FIG. 12(b).

Table 4

Amplitudes and phases of wave-numbers 1 - 10 for 500 mb. field at 41°N for 12Z, 27/12/72.

(a) Met.Office 20 hand-drawn analysis.

(b) Central Forecast Office operational analysis.

Units - decametres, degrees.

Wave-number		1	2	3	4	5	6	7	8	9	10
(a)	Amp.	9.9	6.7	7.6	5.7	1.8	9.8	4.5	.6	2.7	2.4
	Phase	320	132	325	203	90	122	0	194	39	121
(b)	Amp.	8.0	5.0	5.6	3.3	2.6	7.4	2.6	.4	2.9	1.3
	Phase	308	180	304	214	140	110	0	290	59	130

The differences between the two analyses are due mainly to the lack of observations in the Pacific area in the operational analyses. It will be seen that even for very long waves which might have been expected to be relatively little affected by such factors the changes are large. These differences in the initial conditions apparently persist through a substantial part of the forecast.

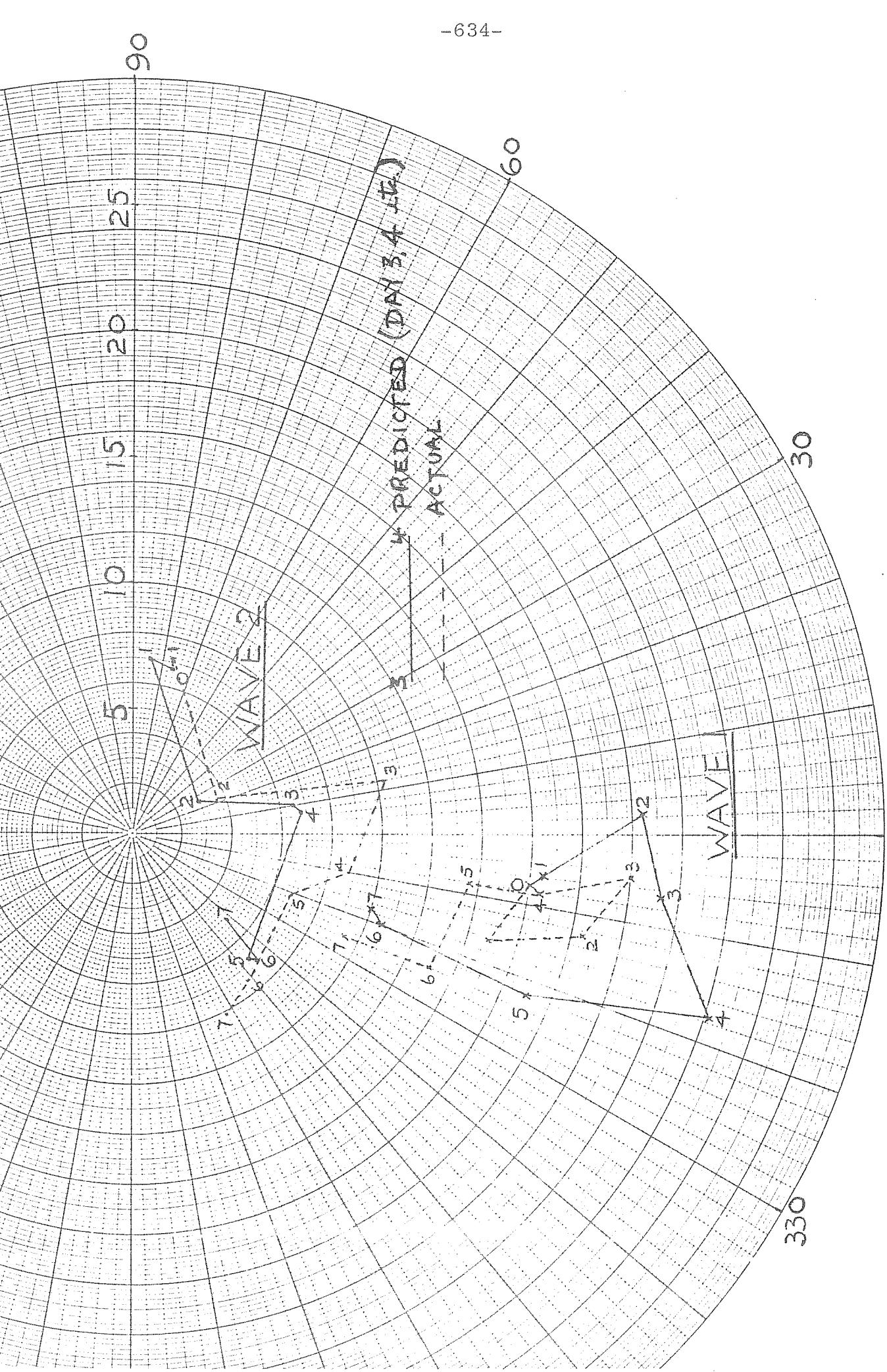

FIG.13 WAVES AT 500MB 51°N JAN 74

The model is not completely lacking in skill in dealing with ultra-long waves, however. For example, fig. 13 shows the amplitude and phase of waves 1 and 2 separately for the second forecast from 4th January 1974 (only two forecasts applying to the winter period have so far been studied in depth). Although the changes from day to day do not correspond precisely with the observed the main change over the period of a few days is reasonably well captured.

Waves 3-5, fig. 11 again show the influence of the differences in the initial data but nevertheless the model appears to handle them fairly well. There is even some evidence that features which are not well dealt with at their inception may nevertheless improve later in the forecast. Thus the ridge at about 80^{o}E and the downstream trough are more realistic towards the end of the integration than in the middle. Also the simulation between about 240^{o}W and 30^{o}W shows the right sort of development though the intrusion of an extra trough and ridge close to the British Isles late in the integration is not reproduced.

Probably the least successful area of the model's prediction capabilities emerges from the diagrams for waves 6-10. Although these appear reasonable in the first few days with the phase speeds well simulated, it is clear that towards the end of the integration development is very weak and the model features bear little resemblance to those of the atmosphere. This lack of realism may

well be connected with the observed tendency for general circulation models to require a too intense zonal circulation to maintain a realistic ratio of eddy to kinetic energy while maintaining also a realistic energy spectrum. In effect there is a period following the first few days when the model is not capable of producing depressions at a realistic rate because the initial available potential energy has either been converted to kinetic energy or has been smoothed (by explicit smoothing to some extent, but this is not enough to account for the observed effects, and other factors such as the dispersion are probably important). If an integration is continued beyond the period considered here, then the available potential energy increases and after 10 - 15 days the model features appear once more to be quite realistic. Bridging this gap between the time the model is feeding on the initial potential energy and the time it achieves something approaching its equilibrium general circulation activity may be one of the most difficult problems in medium-range forecasting.

From the foregoing it will be clear that we are well aware that there is considerable scope for improvement of the model's forecasting capabilities, and it is too early yet to define the real limitations which can be expected from a model of this kind. In order to give some idea of where the main problems lie, the following gives a summary of what appear to be the systematic errors we observe in the model's synoptic evolutions determined on the basis of the relatively few forecasts so far completed.

1. Depressions on the whole but not by any means consistently, move too slowly. This one supposes is due to the use of second order finite differences.

2. Depressions after a day or two tend to be too deep. This seems more due to an extended period of deepening than to deepening at too rapid a rate.

3. The model performs better over the oceans than over land. The tendency for depressions to be too deep is most noticeable over land and the treatment of continental anticyclones leaves a fair amount to be desired.

4. After 6 or 7 days, there is a general lack of synoptic development and an upper flow that is too westerly.

5. The effect of interaction with the earth's surface on synoptic development

The observation that the PMSL values in a forecast are usually more realistic over sea than over a land surface led to an investigation of the surface fluxes or momentum, heat and water vapour and of their influence on the development of a depression.

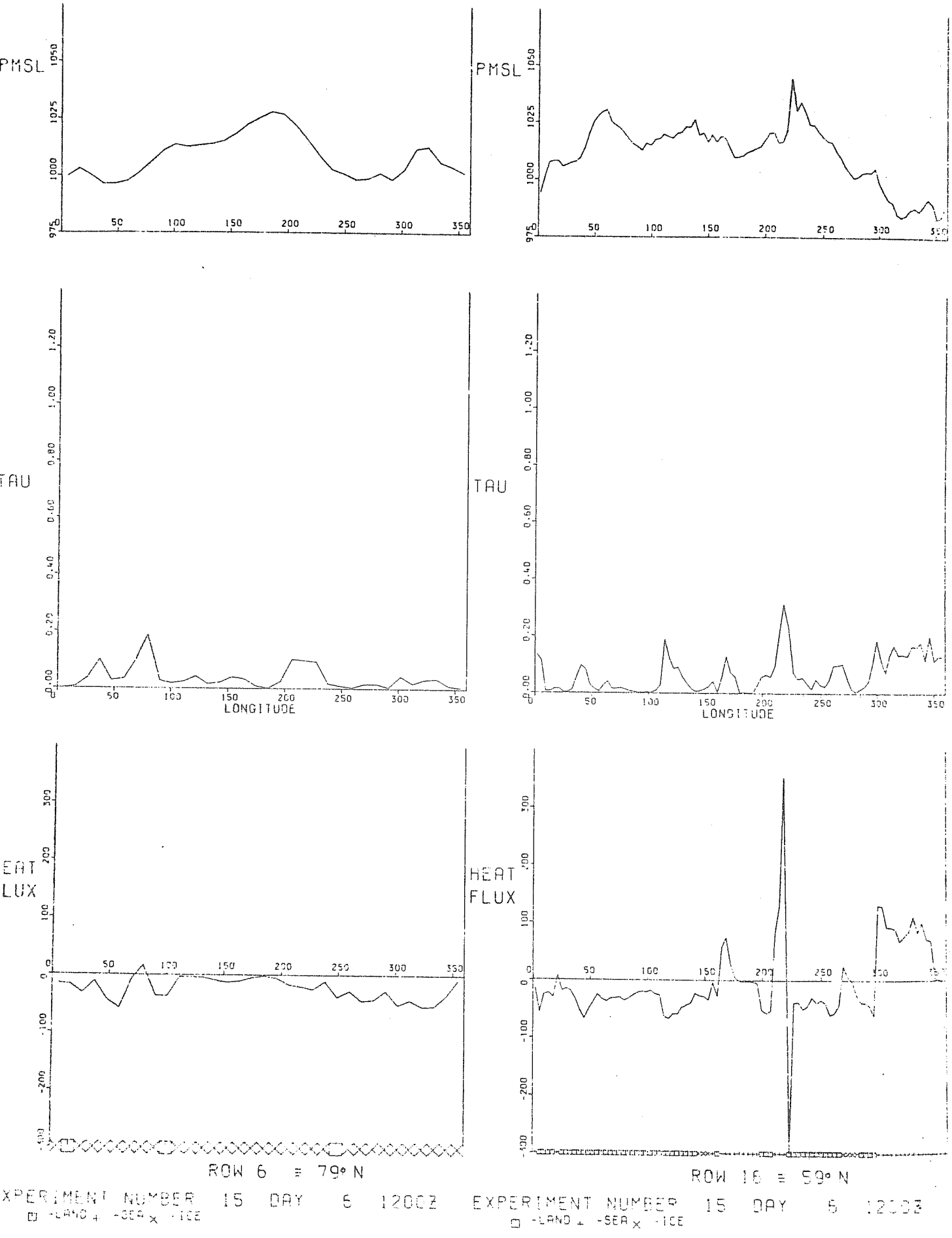
PMSL
1050
1025
1000
975
50
100
150
200
250
300
350
PMSL
TAU
1.20
1.00
0.80
0.60
0.40
0.20
0.00
LONGITUDE
TAU
HEAT FLUX
300
200
100
0
-100
-200
-300
ROW 6 = 79° N
HEAT FLUX
ROW 16 = 59° N
EXPERIMENT NUMBER 15 DAY 5 12003
□ -LAND + -SEA × -ICE
EXPERIMENT NUMBER 15 DAY 5 12003
□ -LAND + -SEA × -ICE

FIG. 14.

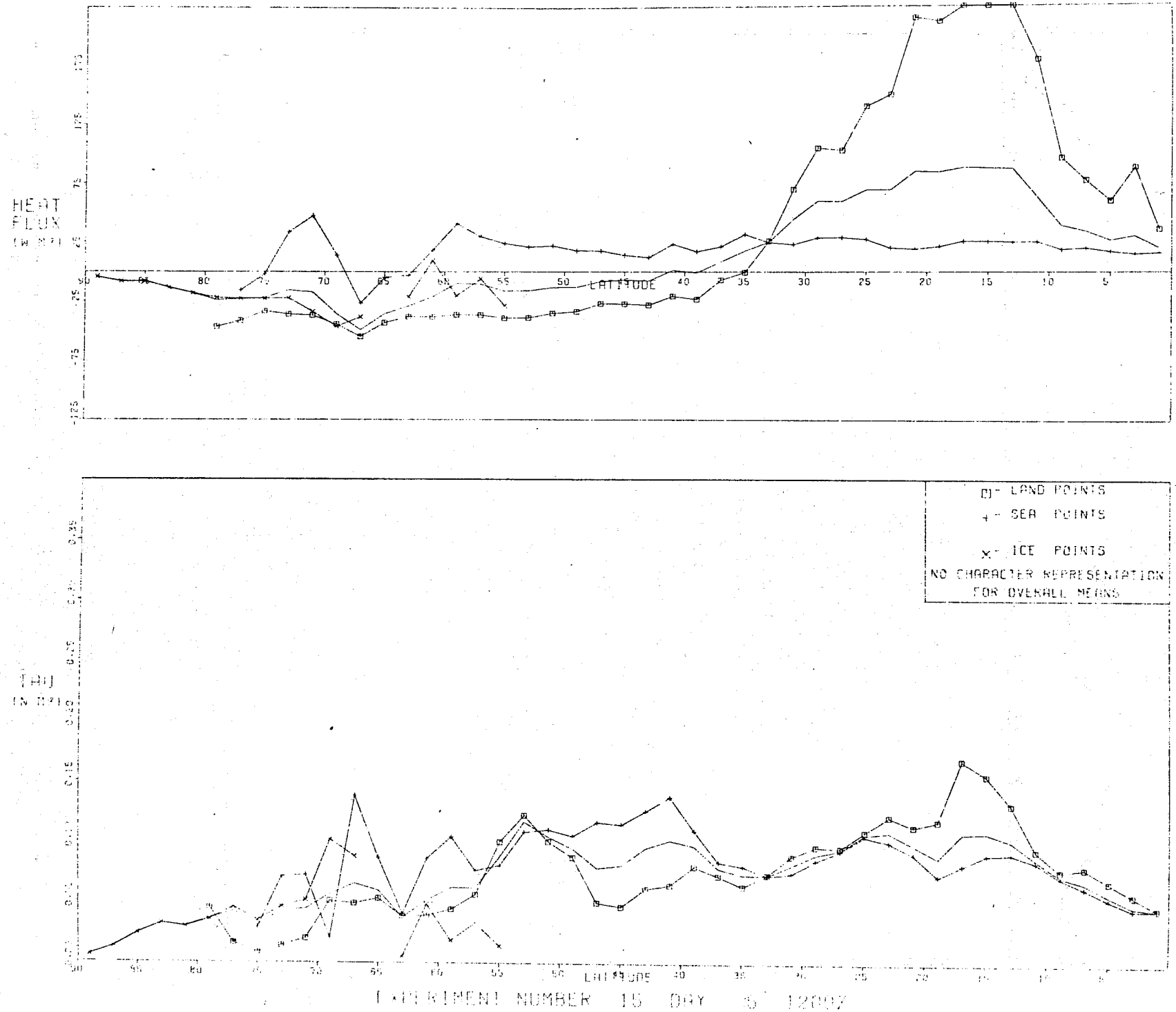
HEAT
FLUX
LATITUDE
0 = LAND POINTS
+ = SEA POINTS
X = ICE POINTS
NO CHARACTER REPRESENTATION
FOR OVERALL MEANS
EXPERIMENT NUMBER 15 DAY 5 1200Z

FIG 15

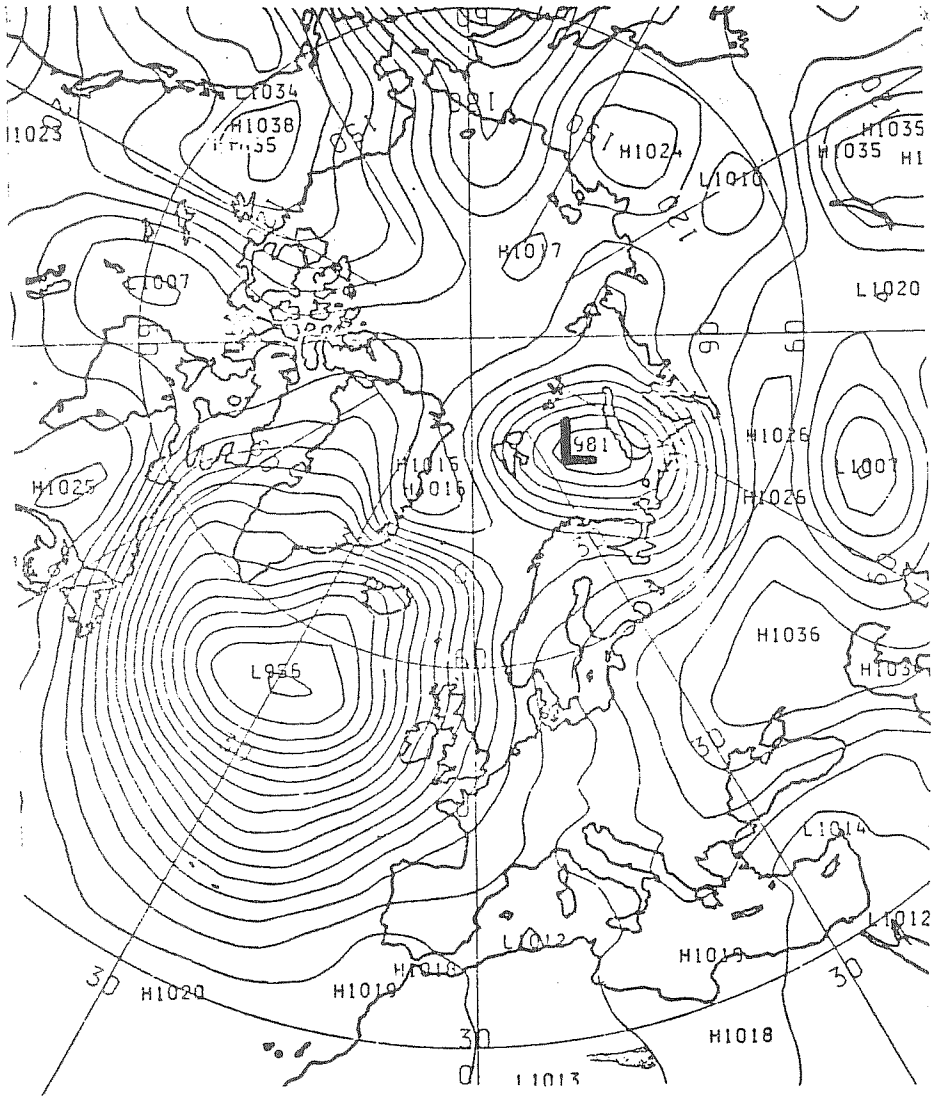

(a)

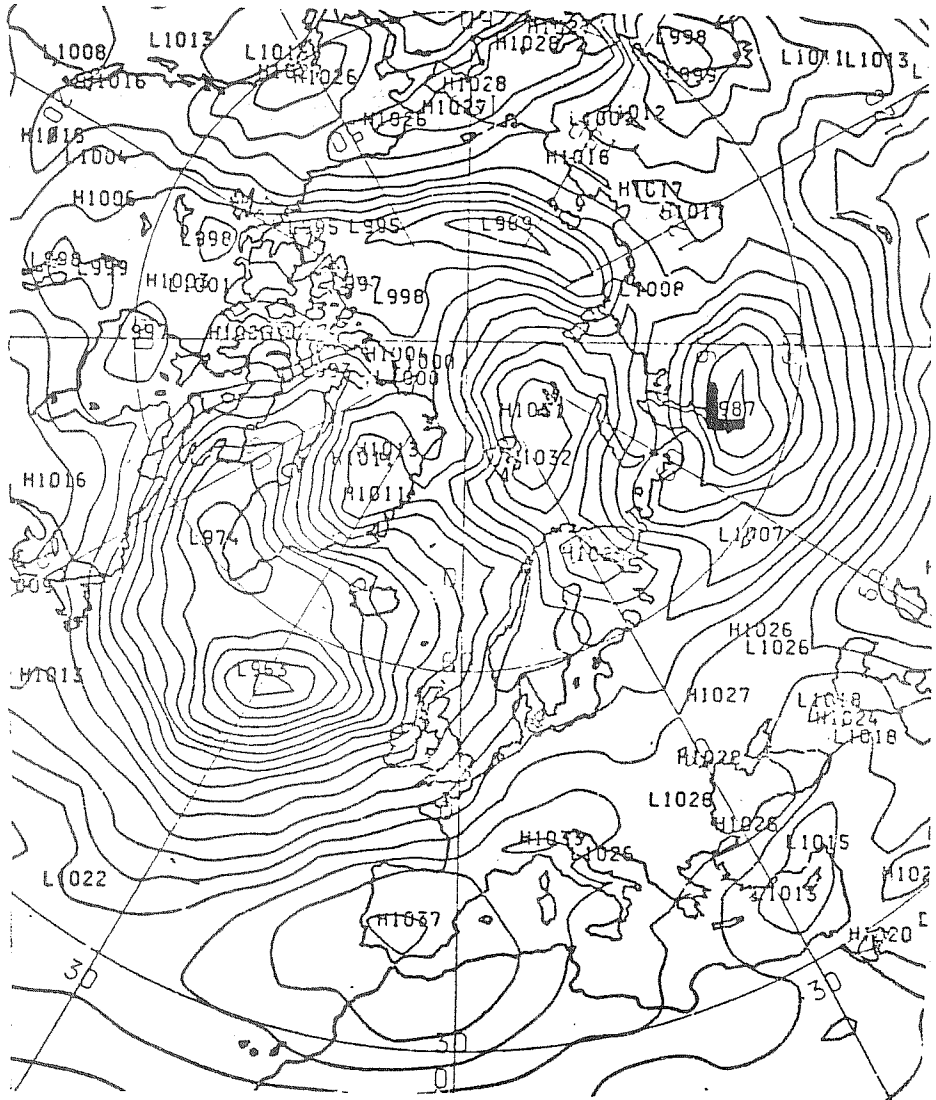

(b)

FIG 16

PMSL D00H00

PMSL D03H06

CONTOUR INTERVAL = 4 MB

Fig. 14 shows for a particular time in a January integration (1) PMSL (2) 'tau', the surface shearing stress and (3) the sensible heat exchange around 79°N and 59°N. The units are respectively millibars, newtons $.m^{-2}$ and watts$.m^{-2}$. There is a tendency for the surface stress and the pressure to be inversely correlated. The most striking feature of the heat fluxes is the massive maximum followed by a large negative value on moving from a relatively warm sea point to the first cold land point. (It may be noted that the extreme values here were a function of the particular synoptic situation and not typical of all land/sea boundaries). Of more important general significance however is the fact that the fluxes over land are negative, and this is so even at local noon at 59°N. The values are fairly large being commonly in excess of -50 watts$.m^{-2}$. Zonal mean heat fluxes and the surface stresses for 12Z are shown in fig. 15 for different types of land surface. All latitudes north of 35°N have negative heat fluxes. Despite this the shearing stress over land remains fairly high. These results indicate that the model is tending to produce strong inversions close to the earth's surface while maintaining strong winds at the lowest level. This combination does not seem altogether realistic and it was thought it might be responsible at least in some measure for the observed tendency for depressions to remain too deep over land. South of 35°N the heat fluxes are positive and rather large; it is to be noted that this is partly because at 12Z there is a large contribution to the land values from the African continent.

A particular depression which failed to fill quickly enough is shown at an initial time of a forecast and 78hr.later in fig. 16(a) and (b). At the latter time its central pressure was 987mb., 26mb. lower than the observed value. The central pressure as observed and as produced by the model in its forecast integration is shown plotted against time in fig. 17, curves (a) and (b) respectively.

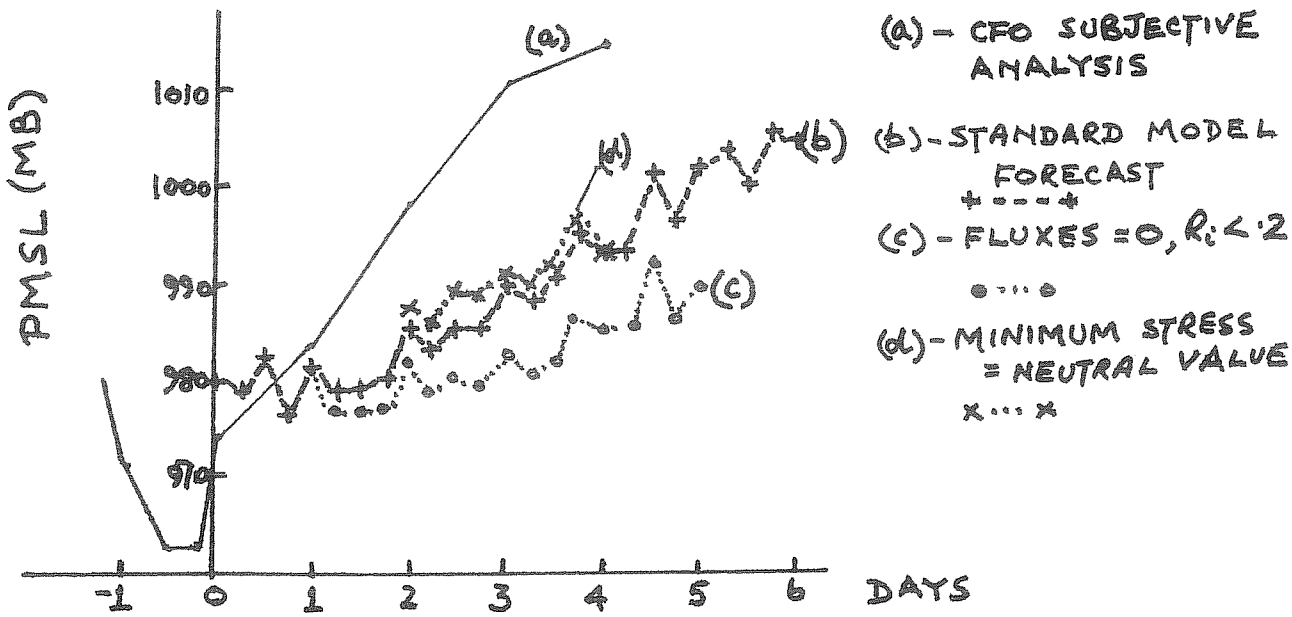

Fig. 17

The diagram shows that the depression reached its greatest depth about 24hr. before the forecast began and thereafter filled rapidly. The model integration caused the depression to become less intense, but at much too slow a rate. Over the Asian continent conditions in the lowest layers were very stable with large downward heat fluxes. This is an interesting

example for which it seemed desirable to carry out an investigation of the effect of heat and momentum exchanges on the synoptic development.

Two experiments have been completed. In the first, the transfer coefficients for heat, water vapour and momentum were set to zero when the bulk Richardson number R_i fell below a critical value of .2. In effect this was assuming that beyond this critical value the air flow over the earth's surface was laminar with all turbulent exchange suppressed by the strongly stable environment. Under such conditions the atmosphere is essentially decoupled from the underlying surface and synoptic development is controlled almost entirely by dynamical factors within the atmosphere. This integration provides a base-line against which to judge the effects of including surface effects. As expected, in this integration the depression filled less slowly than in the original (Fig. 17, curve (c)).

In the second experiment, the same conditions were assumed to apply to heat and water vapour exchanges but the shearing stress was not allowed to fall below its neutral value. This was motivated by the supposition that with strong winds there must be strong mechanical turbulence near the earth's surface and this should lead to a neutral layer; however, since it was thought that the original downward fluxes of heat and water vapour were probably excessive they were not restored to their original formulation.

In this experiment, the depression filled at about the same rate as with the standard form of the model. There is an implication that downward heat and water vapour fluxes are themselves significant in affecting synoptic development.

It is evident that further investigations of this kind are needed to arrive at a greater understanding of the role of the surface exchanges in the model, and indeed it is desirable to enlarge the scope to look at the effect of the boundary layer as a whole on the overlying atmosphere. Work along these lines is proceeding.

6. Experiments with the 5-layer model

I wish now to turn from the results of the 11-layer model to consider some experiments with the 5-layer general circulation model which seem to have relevance to the problems of medium-range forecasting.

6.1 The first experiment was carried out as part of a larger Observing Systems Simulation investigation. In this, one model's results are considered to define the 'truth'; pseudo-observations similar in number, distribution and accuracy to a prescribed global observing system are derived from it and are used in a forecast-analysis cycle with a second model in an attempt to reproduce the atmospheric developments of the first. In effect, the first model plays the part of the real atmosphere while the second is used for

forecasting. The two models in this instance were respectively the 11- and 5-layer, the 11-layer results being taken from a period later in an integration than that at which the flow tends to be too smooth.

Both models are capable of giving reasonable representations of the real atmosphere. The general circulation results from the 5-layer model are fairly realistic (Gilchrist (1974) (1975a)) and even in forecasting mode its results are not grossly inferior to those of the 11-layer model. They differ however in resolution and therefore in truncation error and also in their physical parameterisations. Generally speaking, those of the 5-layer model are simpler.

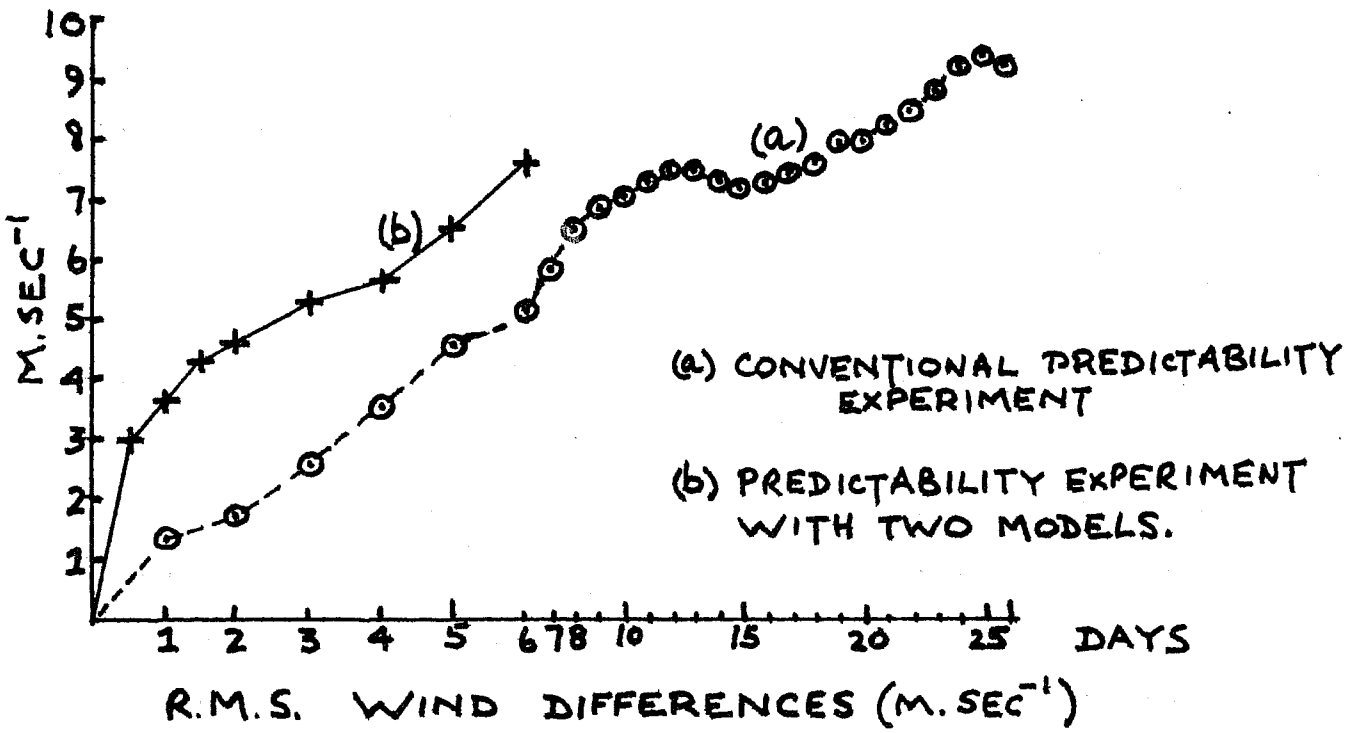

Fig. 18

The broken line in fig. 18 shows the result of a conventional predictability experiment with the 5-layer model. A small random temperature perturbation of up to 2K was added to the initial data, and the r.m.s. wind error between integrations with and without the perturbation was calculated through the integration. The difference between the integrations grows with an initial doubling period of about 2 days, which becomes less with time. At 6 days it is close to 4 days. The rate of increase slackens considerably after about 10 days and the differences are quasi-steady after about 25 days. This curve can be thought of as illustrating theoretical predictability; that is, what could be achieved with a perfect model and a near-perfect observing system.

The solid line in fig. 18 has been obtained by interpolating from an initial set of 11-layer conditions on to the 5-layer model grid and then integrating forward in time from the latter. At each day the error between the 5-layer model forecasts and the 'truth' interpolated onto its grid has been calculated. The growth of differences between the models i.e. the forecast errors, is rapid. It will be noted for example that a difference of 4 $m.sec^{-1}$, which is reached in the normal predictability experiment after $4\frac{1}{2}$ days is here reached in only $1\frac{1}{2}$ days. Of special note too is the very rapid growth of error in the first 12 hours;

this might be fictitiously high due to the lack of proper initialisation and the different balance requirements in the two models, but this can hardly account for all of the difference between the two curves in the initial stages. This experiment provides a more realistic estimate of what is likely to be achieved in practice. The initial conditions, differing from the real atmospheric conditions only in that they have been interpolated on to a wider mesh, must be thought of as close to what might be obtained from a near-perfect observing system, and the errors are therefore due essentially to the inability of one model to simulate precisely what takes place in another.

6.2 The Dynamical Climatology branch has been carrying out a series of experiments one of whose objectives can be thought of as a first attempt to examine the possibility of providing forecasts based on model results applying to a period of about a month ahead. The methodology consists of integrating forward in time with the 5-layer model from real initial conditions for a period of about 50 days (a) with climatological sea-surface temperatures and (b) with sea-surface temperatures containing the anomalies observed at the initial time. The differences between averages taken over the last thirty days or so of the integrations are then compared with the observed anomalies for the appropriate month.

It is not expected that this will provide useful monthly forecasts in the short term. Its immediate importance lies in two other considerations. Firstly,that it provides an ongoing method of comparing the results of a climate model with reality, and therefore one hopes that it will be a method of continuously improving model performance. It may be recalled that very significant improvements in the performance of forecasting models have been made as a result of studying their day-to-day forecasts and it seems imperative to have a similar continuous examination of climate model results if they are eventually to be used for realistic climate prediction. Secondly, climate groups are now acutely aware of the necessity to examine the results of their models in many different circumstances in order to explore the full range of climatologies they are capable of producing. Only if this is known can the results of climatic change experiments be sensibly interpreted. The present experiments provide the opportunity of building up the necessary statistics about the 5-layer general circulation model at the same time as subjecting it to a comparison with reality.

Although it is not to be expected that the integrations will provide useful forecasts immediately, there is evidence that they ought to have some skill; Rowntree (1975 b) has shown integrations of this kind which correctly indicated the main surface pressure anomalies in the Atlantic sector for the winter of 1962-3. An important aspect of the investigation is therefore to determine whether the degree of skill is sufficient to be of practical value.

It will be noted that the experiments differ in two respects from previous experiments on sea-surface temperature anomalies; viz.

(i) the anomalies which are being introduced are not simple and discreet but are inserted for the hemisphere as a whole; they also have their actual values and are not enhanced to artificially increase the model response. It would of course be preferable to use integrations on a global scale but this is not possible at the present time.

It is important for the purposes in mind to put in the observed anomalies over the whole area of integration since it is possible that the atmospheric response to surface temperature forcing as a whole may differ from the sum of its responses to the individual anomalies; there is some indication of this possibility in experiments in which heat was added to the atmosphere at two distinct localities (Gilchrist (1975b)).

(ii) the forecasts are from real initial conditions and although primary interest lies in the average conditions over a period towards the end of the integration, results for the whole period will be examined and compared with reality, particularly to see whether persistent, large-scale atmospheric features are being retained

in the model to a sufficient degree. In particular, there is a possibility that the decline of eddy kinetic energy which occurs at approximately 5 - 15 days will tend to destroy the possibility of producing realistic forecasts, and, if it does, it will be necessary to try to find some way of maintaining the simulation of persistent features through this period.

It is first of all necessary to demonstrate that the method proposed is capable of producing a 'signal' which can be considered to be the forecast. That is, there is a possibility that two integrations with different sea-surface temperatures but identical initial conditions will differ by less than integrations from different initial conditions with the same sea-surface temperatures. If this were the case, it would not be reasonable to treat the differences of the former kind as a forecast since they would be in effect a manifestation of model 'noise'. However, tests which have been carried out by starting the integration off from successive days and comparing the average results over a period of 30 days, have indicated so far that there are systematic and reproducible differences between the 'climatological' and 'anomaly' runs and that therefore there is some justification for treating the difference between the two as a tentative forecast.

An example from this series of experiments may be of interest. In fig. 19 (a) and (b) are shown the 500 mb. contour height reconstructions for latitude $49\frac{1}{2}^{o}$N for wave-numbers 3-5 for days 1 to 51 of an integration started off from real data for 10th September 1974; the sea-surface temperatures were the normal values for September. Fig. 20 (a) and (b) shows the equivalent for a similar integration using the actual sea-surface temperatures for the initial time. The latter were derived mainly from 5-day mean sea-surface temperature charts drawn in the Long Range Forecasting section of the Meteorological Office, though some extension of these to cover the hemisphere was necessary by using additional available observations.

Comparison of fig. 19 (a) and 20 (a) indicates that significant differences caused by the sea-surface temperatures are apparent before 10 days, and large differences are obvious thereafter. The behaviour of the trough at about 180^{o} for example is quite different in the two integrations. With the actual sea-surface temperatures this trough is maintained strongly throughout almost the whole of the 50 days. This feature was evident on the 30-day mean differences between the experiments and was also evident when initial conditions were varied e.g. by starting from the 11th or 12th of the month. Other features which came through as a 'signal' i.e. as consistent differences which seemed not to depend on the initial conditions were that when climatological temperatures were used, there were troughs near the British Isles and at about 70^{o}W they were more intense than in the

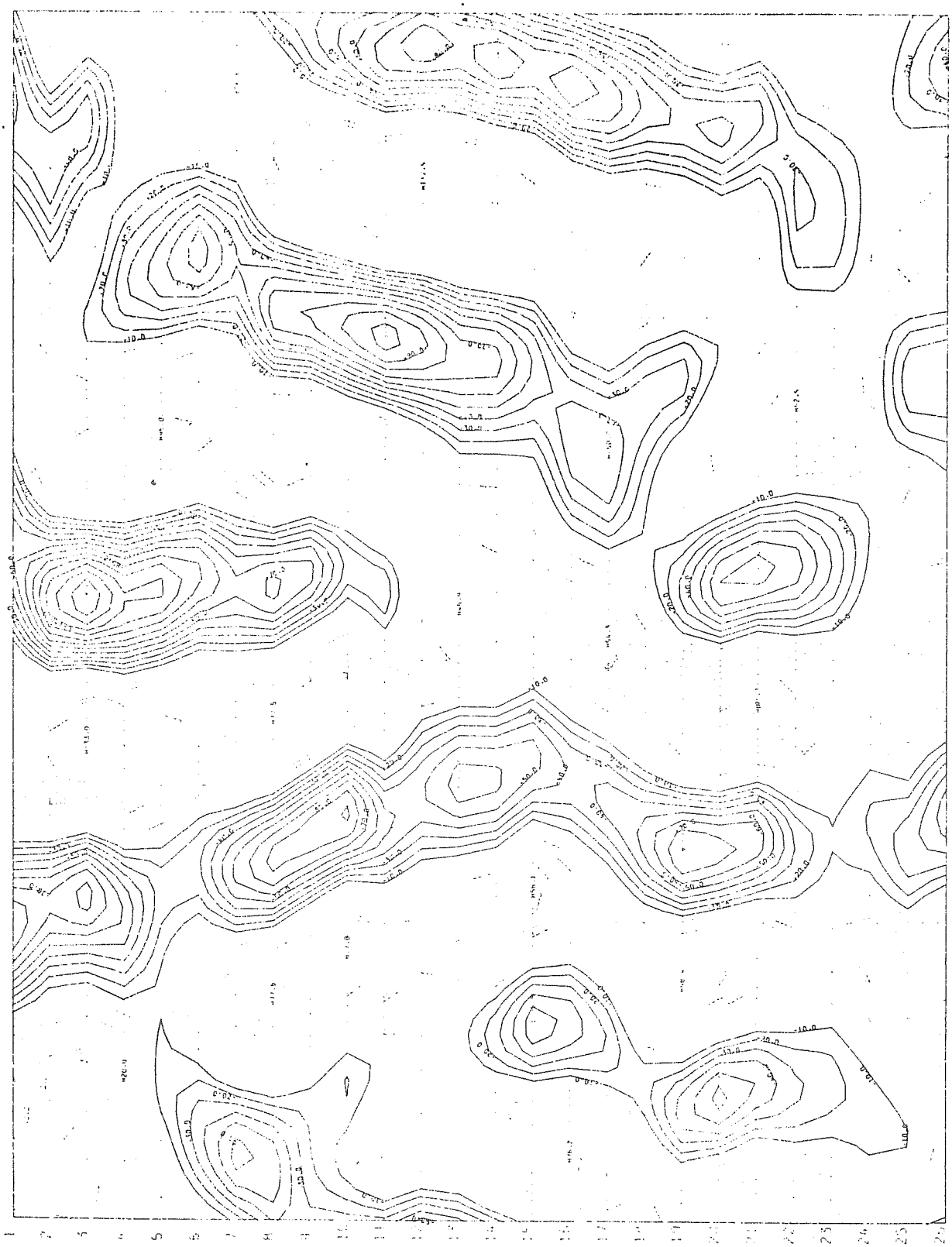
MEAN OF WAVE NOS 3 - 5 AT LATITUDE = 44
DAY = 1 HOUR = 0 TO DAY = 26 HOUR = 0 AT 24 HOUR INTERVALS
CONTOUR INTERVAL = 10.0
LONGITUDE (EAST)
EXPERIMENT NO = 469

FIG. 19(a)

FROM ANALYSIS OF 500MB HTS. (STARTING AT DAY 00)
MEAN OF WAVE NOS 3 - 5 AT LATITUDE = 49
DAY = 26 HOUR = 0 TO DAY = 51 HOUR = 0 AT 24 HOUR INTERVALS
CONTOUR INTERVAL = 10.0
LONGITUDE (EAST)
EXPERIMENT NO = 469

FIG. 10 (L)

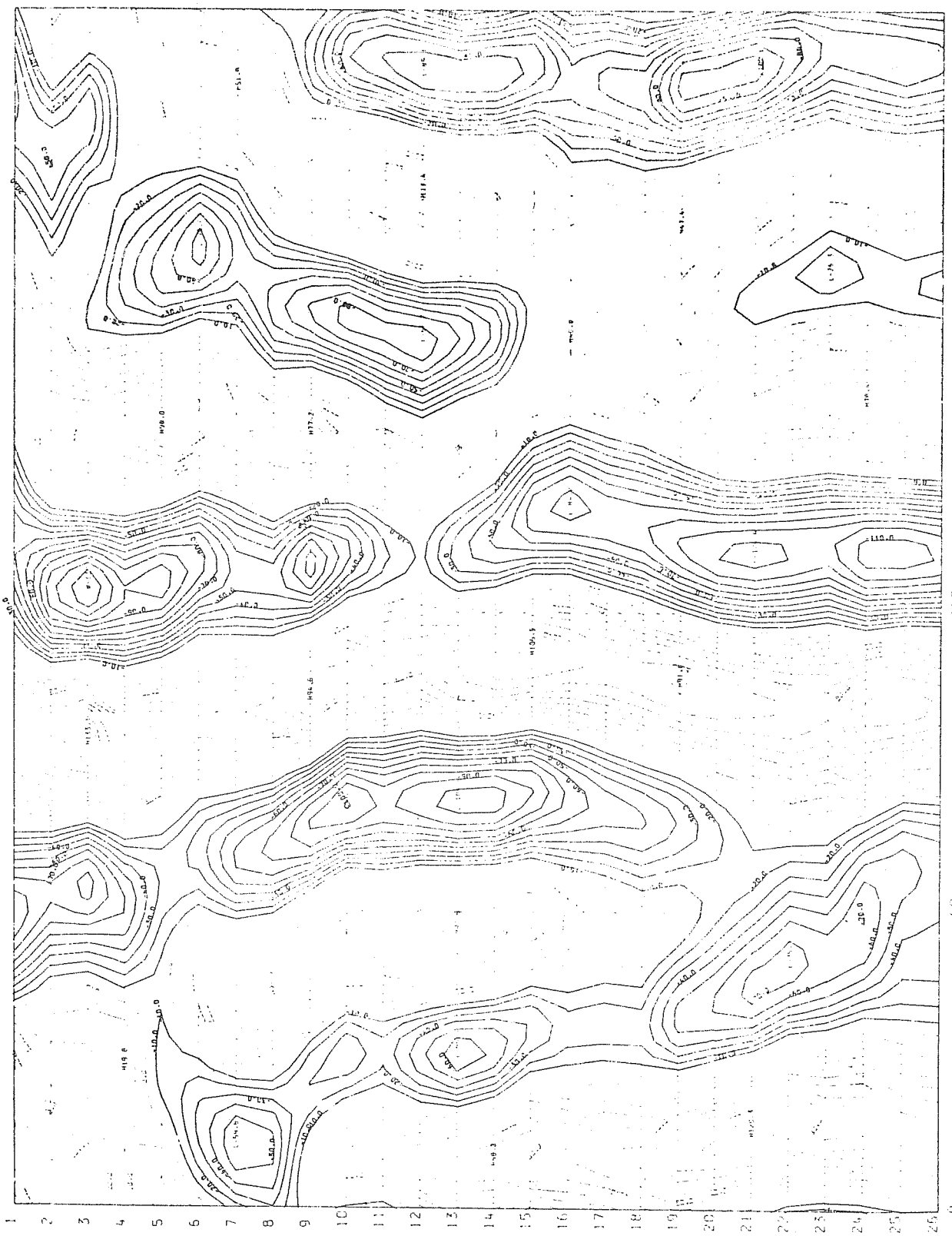
FROM ANALYSIS OF 500MB HTS. (STARTING AT DAY 00)
MEAN OF WAVE NOS 3 - 5 AT LATITUDE = 49
DAY = 1 HOUR = 0 TO DAY = 26 HOUR = 0 AT 24 HOUR INTERVALS
CONTOUR INTERVAL = 10.0
LONGITUDE (EAST)
EXPERIMENT NO = 475

FIG. 20(a)

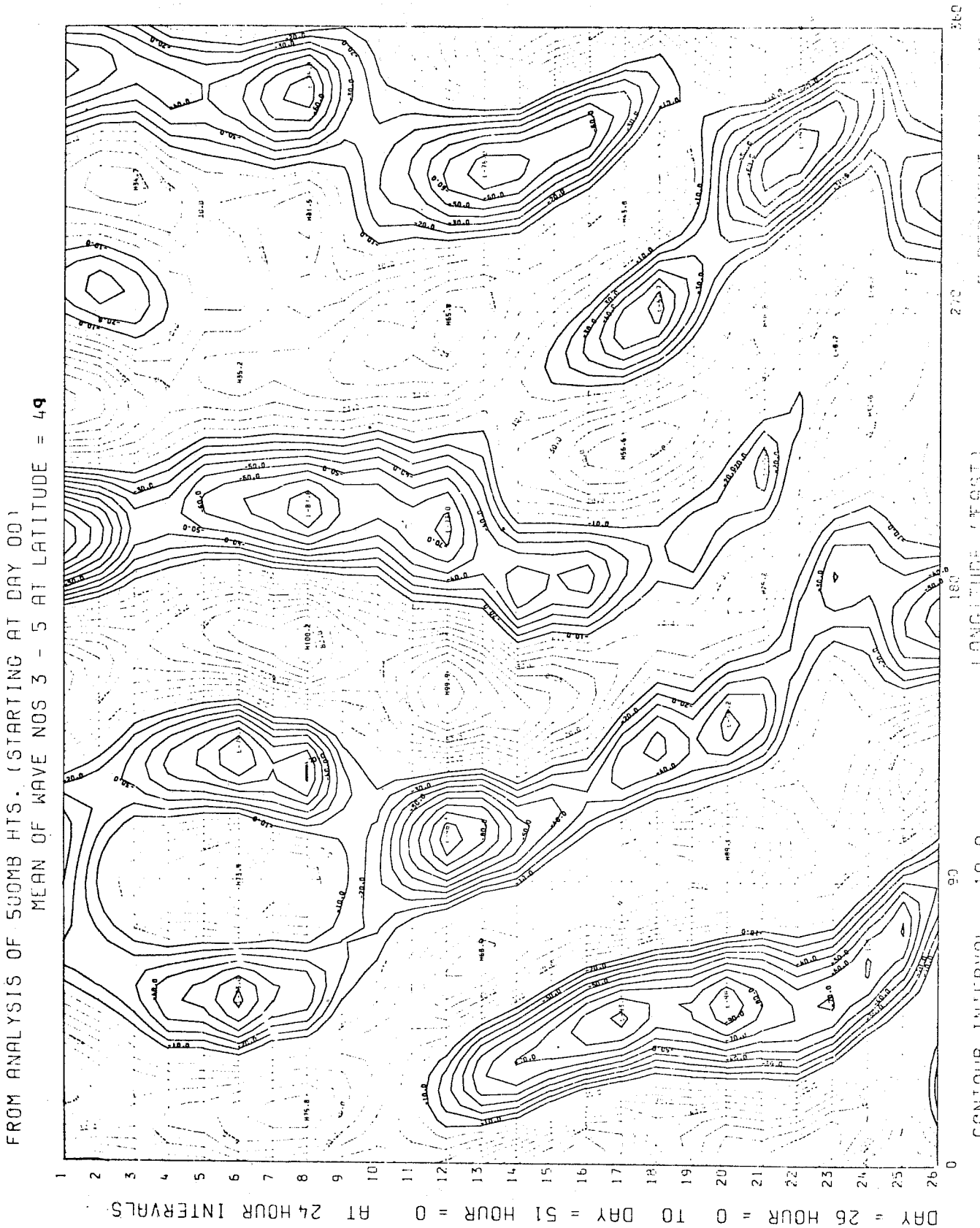
FROM ANALYSIS OF SUOMB HTS. (STARTING AT DAY 001)
MEAN OF WAVE NOS 3 - 5 AT LATITUDE = 49
DAY = 26 HOUR = 0 TO DAY = 51 HOUR = 0 AT 24 HOUR INTERVALS
CONTOUR INTERVAL = 10.0
LONGITUDE (EAST)
EXPERIMENT NO. 715

FIG. 20(b)

'anomaly' integrations.

Integrations of the kind I have been considering have only just reached the stage at which they can begin to be examined in depth. Obviously much remains to be done before they can approach the state where it is reasonable to expect them to be producing forecasts of any practical value. They represent however an important stage in the process which has to be gone through in order to achieve that goal.

7. Acknowledgement

In preparing these lectures I have been able to draw freely upon the work and the advice of the staff of the Dynamical Climatology branch of the Meteorological Office, for whose cooperation I am most grateful.

References

Asselin, R. 1972 'Frequency filter for time integrations' Monthly Weather Review 100 pp. 487 - 490

Bryan, K. 1966 'A scheme for numerical integration of the equations of motion on an irregular grid free of non-linear instabilities' Monthly Weather Review 94 pp. 39 - 40

Clarke, R.H. 1970 'Recommended methods for the treatment of the boundary layer in numerical models' Australian Met. Mag., 18 No.2 pp. 51 - 73

Corby, G.A. Gilchrist, A. & Newson, R.L. 1972 'A general circulation model of the atmosphere suitable for long period integrations' Quarterly Journal Met. S. 98 pp. 809 - 832

Gilchrist, A. 1974 'General circulation model of the atmosphere incorporating an explicit boundary layer top' Meteorological Office 20 Tech. Note II/29

1975a 'Tropical results from a July integration of a general circulation model incorporating an explicit boundary layer top' Meteorological Office 20 Tech. Note II/46 (in preparation).

1975b 'Two climatic change experiments' Meteorological Office 20 Tech. Note II/50

Grimmer, M.S. & Shaw, D.S. 1967 'Energy conserving integrations of the primitive equations on the sphere' Quarterly Journal Royal Met.S. 93 pp. 337 - 349

Hunt, G.E. & Mattingly, S.R. 1974 'Atmospheric radiation studies' Meteorological Office 20 Tech. Note II/31

Kurihara, Y. 1965 'Numerical integration of the primitive equations on a spherical grid' Monthly Weather Review 93 pp. 399 - 415

Lyne, W.H. Rowntree, P.R. Temperton, C. & Walker, J.M. 1975 'Numerical modelling during GATE' Meteorological Office 20 Tech. Note II/37

Manabe, S.& Möller,F. 1961 'On the radiative equilibrium and heat balance of the atmosphere' Monthly Weather Review 89 pp. 503 - 532

Newson, R.L. 1974 Proceedings of 3rd Conference on CIAP pp. 461 - 473

Rowntree, P.R. 1971 'Proposed vertical resolution in a new Meteorological Office 20 model' Meteorological Office 20 Tech. Note II/1

Rowntree, P.R. 1975a 'Tropical forcing of atmospheric motions'
Meteorological Office 20
Tech. Note II/48

1975b 'Response of the atmosphere to a tropical Atlantic temperature anomaly'
Meteorological Office 20
Tech. Note II/49

Saker, N.J. 1974a 'An 11-layer general circulation model'
Meteorological Office 20
Tech. Note II/30

1974b 'Some results from the first forecasting experiment using the Meteorological Office 20 high resolution model'
Meteorological Office 20
Tech. Note II/26

1974c 'A high resolution model experiment - initial conditions 4/1/74'
Meteorological Office 20
Tech. Note II/32

Shapiro, R. 1971 'The use of linear filtering as a parameterisation of atmospheric diffusion' Journal of Atmospheric Sci. 28 pp. 523 - 531

Shuman, F.G. 1970 'On certain truncation errors associated with spherical co-ordinates' Journal Appl. Met. 9 pp. 564 - 570

Smagorinsky, J. Manabe, S. & Holloway, J.L.J. 1965 'Numerical results from a nine-level model of the atmosphere' Monthly Weather Review 93 pp. 727 - 768

Temperton, C. 1975 'Dynamic initialisation for barotropic and multi-level models' Meteorological Office 20 Tech. Note II/39